CW MID-INFRARED NH_3 LASERS

CW MID-INFRARED NH_3 LASERS

By

DAVID FRANCIS KROEKER, B.Sc.

A Thesis

Submitted to the School of Graduate Studies

in Partial Fulfilment of the Requirements

for the Degree

Master of Science

McMaster University

March 1986

MASTER OF SCIENCE (1986) McMASTER UNIVERSITY

(Physics) Hamilton, Ontario

TITLE: CW Mid-Infrared NH_3 Lasers

AUTHOR: David Francis Kroeker, B. Sc. (Carleton University)

SUPERVISORS: Professor J. Reid and Professor P.E. Jessop

NUMBER OF PAGES: xi, 69

ABSTRACT

This thesis describes a series of experiments that were undertaken to extend the limits of output power and wavelength coverage of optically pumped mid-infrared lasers. Initially, two new cw Raman lasers operating at wavelengths of 11.5 and 12.5 μm were developed. Maximum output powers of 650 and 150 mW were produced, with pump powers of 11 and 3.3 W, respectively. The effect of the pump offset on the output power was then determined by measuring the efficiency of an NH_3 laser pumped at frequency offsets of 94 and 274 MHz. In lasers operating in pure NH_3 the larger pump offset required a greater pump intensity to reach threshold, but efficiency increased with pump offset. Higher NH_3 pressures could be used at larger pump offsets and the improved efficiency was attributed to reduced saturation effects at the higher operating pressures.

Experiments carried out with NH_3 inversion lasers have greatly increased the output powers available at a large number of wavelengths in the 10 to 14 μm range. In a buffered NH_3 mixture, the sR(5,0) transition was pumped on resonance. Collisions with either N_2 or Ar buffer gases were effective in thermalizing the rotational populations in the ν_2=1 vibrational level and producing gain on a wide range of frequencies. Output powers as large as 3.5 W on a single line and

greater than 5 W multi-line were produced, at efficiencies of 20 and 30 % respectively. The number of lasing wavelengths increased substantially, as more than forty ortho-NH_3 transitions were observed to lase in a grating-tuned cavity. The optical pumping technique was then used for the first time to produce line-tunable lasing on para-NH_3 transitions. The sR(5,1) transition was pumped near resonance and 24 para-transitions were observed to lase. In total, lasing was achieved on 65 different transitions in $^{14}NH_3$, with wavelengths of 10.3 to 13.8 μm.

ACKNOWLEDGEMENTS

I wish to thank my principal supervisor, Dr. John Reid, for the challenge and opportunity of working with him. Thanks are also due to my colleagues Claude Rolland and Hugh Morrison, who developed the computer models of gain that are described in chapter 2, and to David Danagher for his critical comments and suggestions regarding this thesis.

TABLE OF CONTENTS

LIST OF FIGURES

LIST OF TABLES

CHAPTER 1

INTRODUCTION

Much research has been undertaken over the last 25 years to produce sources of coherent radiation at wavelengths from the ultraviolet to the far-infrared. Thousands of transitions have been observed to lase, with outputs at wavelengths as short as 0.14 μm and as long as 1200 μm.[1] However, the number of lasers with efficiencies greater than 1 % is a very small fraction of this total. There is an ongoing search for high-intensity sources in areas of the spectrum that have particular scientific interest. One such region is the mid-infrared (5 to 50 μm), where until recently there were few powerful lasers. The vibrational-rotational transitions of many molecules occur in this spectral region. Mid-infrared sources would be of value in measuring the spectroscopic properties of gases and in the detection of trace gases in the atmosphere. Photochemical applications for industry are developing as quickly as new lasers are produced and the possibility of using infrared lasers for isotope separation has also stimulated the development of mid-infrared lasers.

For any type of lasing it is necessary that the gain medium be excited to a non-equilibrium state. This excitation is often provided either by an electrical discharge or by optical pumping. In gas

discharges, collisions between electrons and the gas molecules transfer energy to the vibrational modes of the gas. If a population inversion is created between two states then lasing will occur. In the CO_2 laser, the initial excitation of N_2 is provided by an electrical discharge and the laser gas is excited by the resonant transfer of energy from N_2 to CO_2. In general, electrical excitation is not an efficient process, but the CO and CO_2 lasers, which operate at 5 and 10 μm respectively, are exceptions to the rule. An electrical-to-optical power conversion efficiency of greater than 40 % has been produced in a cw CO laser[2] and 15 % is typical of CO_2 lasers.[1] At other infrared wavelengths there are few electrically-excited lasers of significant power or efficiency.

Optical pumping is one of the pioneering techniques used to produce lasing. The first laser consisted of a ruby rod that was optically pumped by a flashlamp. Current high-power Nd:YAG lasers are similarly pumped, with efficiencies of a few percent. In optical pumping, a molecule absorbs a photon at one frequency and emits a new photon at a second frequency. This pumping method is generally inefficient because the radiation from a flashlamp covers a broad spectral range and only a small fraction of the pump energy is absorbed by the transition of interest. However, in principle almost any molecule can be made to lase if it is pumped with sufficiently intense radiation of the appropriate frequency. High efficiency can be attained if the pump radiation is monochromatic, i.e., if an existing laser is used as a pump. As each of the major discharge-excited lasers was developed, it was used to pump a large number of materials and produce

fluorescence or lasing at other wavelengths. CO_2 has been one of the most important sources for optical pumping because it can operate on a single line and still deliver high power at a large number of wavelengths from 9 to 11 μm.

The optical pumping of NH_3 and other molecules of low molecular weight is a very effective way to convert CO_2 radiation to wavelengths of 10 to 1000 μm. The ν_2 vibrational-rotational frequencies of NH_3 overlap those of the CO_2 9-μm and 10-μm bands and the NH_3 molecule interacts strongly with electromagnetic radiation. The narrow spectral widths and wide spacing between NH_3 transition frequencies ensure that only the transition that is pumped will absorb the pump radiation. However, the highly specific nature of optical pumping has the disadvantage that very close coincidences between the pump and absorber frequencies are required. Such coincidences are rare in an individual absorbing molecule, but a large number of molecules have transitions that are close to the frequencies of CO_2 laser lines. Pumping such molecules has produced far-infrared (FIR) lasing on numerous wavelengths from 50 to 1250 μm in both pulsed and cw systems.[3,4] FIR lasing takes place between rotational states in an upper vibrational level of the pumped molecule. There is generally little population in the upper levels, so it is relatively easy to create an inversion and generate lasing at these frequencies. Mid-infrared (5 to 50 μm) lasing occurs between two different vibrational levels and is much more difficult to achieve. In 1976 Chang and McGee observed lasing at 12.81 μm when they pumped NH_3 with a pulsed laser operating on the CO_2 9R(16) line.[5] The

power of the 12-μm laser has since increased considerably and power conversion efficiencies of 28 % have been reported.[6] Lasing on a wide range of wavelengths was achieved when the CO_2 9R(30) line was used as a pump[7] and power conversion efficiencies of 10 to 20 % have been reported.[8]

In a continuous-wave (cw) system, the use of narrow-bore waveguides in the NH_3 laser cavity has produced results similar to those of the pulsed laser systems. Intensities as high as 10^3 W/cm^2 can be produced by focussing the output of a conventional low-pressure CO_2 laser into a waveguide. Lasing is possible on individual NH_3 transitions when the appropriate CO_2 pump frequencies are used.

Much of the earlier work on cw optical pumping used the CO_2 9R(30) laser line to pump the NH_3 sR(5,0) transition. Output powers as great as 10 W at 12.08 μm and power conversion efficiencies of 28 % were observed.[9] At pump frequency offsets greater than 100 MHz the gain in an optically pumped laser is created by a scattering process. The initial experiments described in this thesis examined the effect of pump offset on the performance of mid-infrared lasers. Three transitions in NH_3 were pumped at different frequency offsets. The frequency of the 9R(30) CO_2 line is 184 MHz higher than that of the NH_3 sR(5,0) transition.[10] As Raman gain has been found to increase with decreasing pump offset, it was decided to pump two transitions that have closer coincidences with CO_2 laser lines. A CO_2 sequence laser, operating on either the 9P(7) or the 9P(17) line, was used to pump the aR(5,1) or the sR(3,3) transition respectively, and the 12-μm output powers and

efficiencies were compared with those of the sR(5,0) system. An experiment was then undertaken to clearly determine the effect of pump offset. The 9R(30) pump line was used in conjunction with an acousto-optic modulator (AOM) to pump the sR(5,0) transition at different frequency offsets. It was found that, while lasing threshold could be reached at low pump powers when the pump offset was small, high efficiency was more characteristic of larger pump offsets. The reason for this behavior and its implication for Raman lasers in general are discussed in chapter 3.

Once the work with Raman lasers was concluded, experiments were carried out to investigate the more versatile NH_3 inversion laser. In 1984, Rolland et al. demonstrated that line-tunable operation could be achieved using a cw pump laser.[11] The inversion laser produced radiation on a large number of wavelengths from 11 to 13 μm when a single transition was pumped. In this respect it is far superior to the Raman laser, which produces output on only the one transition directly coupled to the pumped transition. However, for a population inversion to be created it is necessary that an NH_3 transition be pumped on resonance. A pair of AOMs were used to shift radiation from the CO_2 9R(30) line into coincidence with the sR(5,0) transition in $^{14}NH_3$. In $^{15}NH_3$, the aR(2,0) transition can be effectively pumped by the CO_2 10R(42) line without a frequency shift.[12] Line-tunable lasing has been produced with powers as high as 700 mW in $^{14}NH_3$ and 1.5 W in $^{15}NH_3$.[11,12]

This thesis describes recent experiments that have yielded higher power (>5W) and efficiency (>30 %) in line-tunable NH_3 lasers.

The number of observed lasing wavelengths has increased substantially and the first achievement of cw line-tunable lasing on para-NH_3 transitions is reported. As there is no significant transfer of energy from ortho-NH_3 to para-NH_3, it was necessary to pump a second transition, the sR(5,1) line, in order to produce lasing on para lines. Two thirds of NH_3 lines are para-transitions and the extension of lasing to these transitions will mean much more thorough coverage of the 11-μm to 14-μm region.

The remainder of this thesis consists of four chapters. Chapter 2 sets forth the general spectroscopic properties of NH_3 that are relevant to the development of a mid-infrared laser. The physical processes that contribute to the Raman and inversion gain are described, as are the major features of the computer models used to calculate the gain. Chapter 3 gives an account of the experimental investigations of the Raman laser and of the effect of pump offset on laser efficiency. The operation of two new cw Raman lasers is described and the differences in performance of the sP(7,0) laser at pump offsets of 94 and 274 MHz are examined and explained. Chapter 4 presents the improvements that were observed in the cw line-tunable NH_3 laser when greater pump powers were used. The effectiveness of argon as a buffer gas is compared with that of nitrogen and the achievement of line-tunable operation on para transitions in NH_3 is reported. The performance of the line-tunable laser is evaluated in light of the predictions of a simple model described in chapter 2. Finally, chapter 5 summarizes the discoveries made in this work, the improvements in the

output characteristics of the cw NH_3 laser, and some present and future applications of the line-tunable laser.

CHAPTER 2

THEORY

2.1 Introduction

This chapter presents a brief review of the vibrational and rotational spectroscopy of NH_3. The gain processes that take place when low-pressure pure NH_3 is optically pumped are described in the section on Raman gain. The results of calculations are presented to evaluate the possibility of achieving Raman lasing on selected pump/lasing transitions. Additional effects that are observed when higher-pressure mixtures are pumped on resonance are described in the subsequent section on inversion gain. Some predictions about the behavior of line-tunable NH_3 lasers are then made on the basis of simple theoretical calculations.

2.2 Spectroscopy of NH_3

NH_3 is a pyramidal molecule with threefold rotational symmetry. It has four vibrational modes, two symmetric and two asymmetric. The ν_2 fundamental mode has the lowest energy of the four,[13] and its vibrational-rotational lines overlap the 9-μm and 10-μm bands of CO_2. The ν_2 mode is symmetric, i.e., it preserves the rotational symmetry of the NH_3 molecule. The NH_3 molecule possesses additional symmetry

because its spectroscopic properties do not depend on the orientation of the nitrogen nucleus with respect to the hydrogen plane. If the nitrogen atom were confined to one side or the other, the reflection symmetry would make each vibrational level doubly degenerate. However, the potential barrier at the hydrogen plane is finite, and the nitrogen atom can tunnel through. There is a mixing of the two spatial states to form the s (symmetric) and the a (asymmetric) states. The a state is higher in energy than the s state by 0.8 cm^{-1} in the ground ($\nu_2 = 0$) level, and by 36 cm^{-1} in the $\nu_2=1$ level.[13]

In addition to the energy from vibrational modes, the NH_3 molecule also possesses energy that is stored in its rotational motion. In the absence of an external field, the rotational energy depends only on the quantum numbers J and K, where $K = |k|$ is the projection of the angular momentum J on the axis of symmetry of the molecule. To first order, the rotational energy is $E = BJ(J+1) + (C-B)K^2$, where B and C are constants that are determined by the moments of inertia of the molecule.[13]

The selection rules for electric dipole transitions in the infrared are[14]

$\Delta K = 0$ and $\Delta J = -1, 0, \text{ or } 1$ if $K \neq 0$,

$\Delta J = \pm 1$ if $K = 0$.

In addition there must be a change of symmetry, i.e., a-->s or s-->a. Therefore any vibrational-rotational transition can be specified by the notation xY(J,K), where x is a or s, and Y is P,Q, or R, depending on whether J changes by J = 1, 0, or -1 in going from the upper to the

lower level. The values x, J, and K are those of the lower level.

It is sometimes necessary, for example in electrical discharges, to consider the electronic states of the NH_3 molecule. However, the 9-μm photons used to pump NH_3 have much less energy than is required to excite the molecule to higher electronic states, so only the ground electronic state must be considered in optically pumped NH_3 lasers.

2.3 Gain Processes

2.3.1 Raman Gain

Optical pumping has proved to be a reliable and efficient way to produce gain in the 12-μm region. When pumping with a laser there are usually only three levels that must be considered in gain calculations. In this thesis, all optically pumped laser systems take the form of an inverted "vee", as shown in Figure 2.1. The three levels are the lower levels of the pump and probe transitions and the common upper level. If there is a small offset (< 90 MHz) between the pump frequency and the line center of the NH_3 absorption, then the pump radiation will be absorbed and the molecule excited to the upper level. If a population inversion is created between levels 0 and 1, then stimulated emission can be produced at the line center frequency Ω_{01}. As the pump offset increases, fewer NH_3 molecules absorb the radiation, and little population is transferred to the upper level. A strong absorption exists at line center of the 0-1 transition, but a two-photon scattering process can create gain at nearby frequencies. In the Raman process, a photon of frequency ω_p is converted into one of frequency ω_s. The

FIGURE 2.1 Diagram of the principal energy levels involved in the generation of Raman gain. A pump photon of frequency ω_p is offset by a frequency difference δ_p from Ω_{02}. Gain is measured at a frequency ω_s offset by δ_s from Ω_{01}. The Raman resonance condition is $\delta_s \simeq \delta_p$.

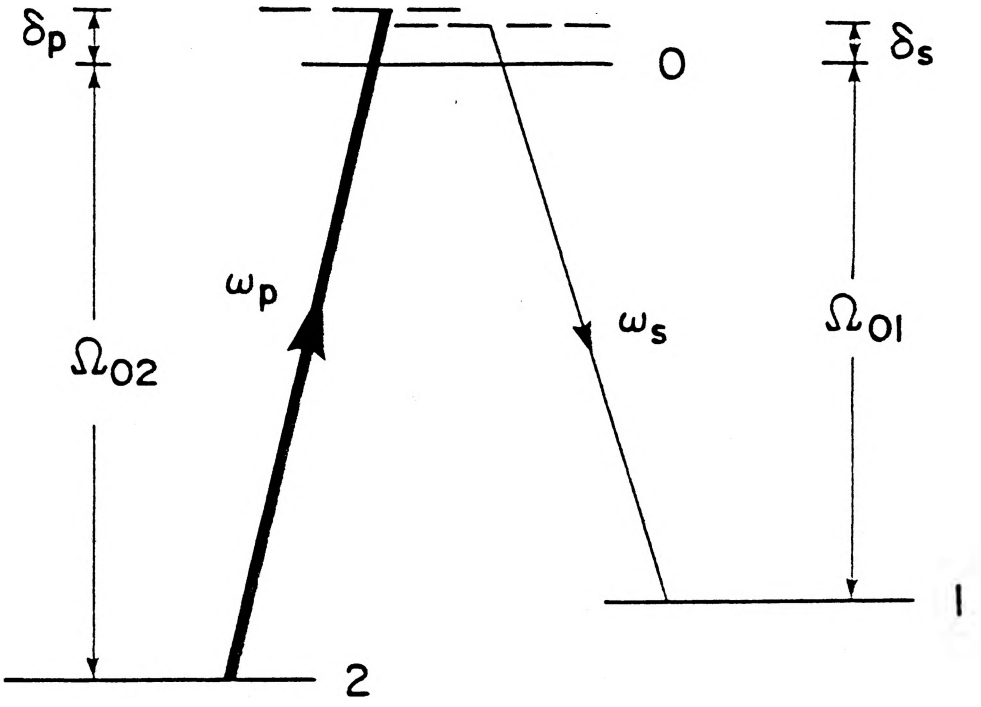
δ_p
δ_s
0
ω_p
ω_s
Ω_{02}
Ω_{01}
1
2

frequency change corresponds to the energy difference between the molecular levels 1 and 2. The scattered photon will have a frequency offset from Ω_{01} that is roughly equal to the pump offset. Inversion gain requires pumping near resonance ($\delta_p \simeq 0$), whereas the two-photon nature of the Raman process ensures that, even at fairly large pump offsets, the Raman resonance condition $\delta_s \simeq \delta_p$ can be satisfied. For convenience, the pump and scattered radiation are labelled with the spectroscopic notation of the nearby NH_3 transitions. It should be kept in mind that this notation does not signify that an absorption/emission process takes place, but merely indicates the levels that are involved in the resonant Raman process. The selection rules for Raman transitions are[14]

$$\Delta K = 0 , \quad a \text{-->} a \text{ or } s \text{-->} s$$

$$\text{and } \Delta J = 0, \pm 1, \pm 2 \quad \text{if } K \neq 0 ,$$

$$\Delta J = 0, \pm 2 \quad \text{if } K = 0.$$

The Raman gain is proportional to the population difference between levels 2 and 1. Generally the population in the vibrational-rotational levels of NH_3 decreases with J, thus maximum gain will be produced on the coupled P-transition when an R-branch transition is pumped ($\Delta J = 2$). In thermal equilibrium there is a larger population in level 1 than in level 2. Consequently, it is much easier to generate gain at low pump intensities by the Raman process than by creating a population inversion between levels 0 and 1.

Theoretical descriptions developed by Panock and Temkin[15] and Heppner *et al.*[16] to describe the gain processes in optically pumped

far-infrared lasers have been found to work equally well for mid-infrared lasers. This theory was the basis for the computer model that was used to make the gain calculations for this thesis. Details of the calculations have been given by Morrison[17] and Rolland[18] and will not be repeated here. The model employs a density matrix formalism and considers only the three levels shown in Figure 2.1. The cw case is assumed, i.e., the populations in the three levels are assumed to have reached a steady state. The standard rotating wave approximation is used for the polarization terms in the density matrix and numerical methods are used to calculate the Raman and inversion gains.

The computer model describes many characteristics of Raman gain that have been observed by Rolland et al.[19,20] In several experiments, a tunable diode laser was used to probe the gain in optically pumped NH_3. When the pump and probe propagated in the same direction (copropagated) the gain was found to have a width equal to the difference between the Doppler absorption linewidths of NH_3 at the pump and probe frequencies. The width of the counterpropagating gain was equal to the sum of the Doppler widths and the peak gain was correspondingly smaller than that observed in the copropagating case. It was also confirmed experimentally that the small-signal gain scales linearly with the pump intensity.

In this work, the computer model was modified to make it suitable for calculating the gain for any pair of coupled R-P (absorption-emission) transitions in NH_3. The three transitions that were optically pumped in the experiments described in chapter 3 are the

sR(5,0), sR(3,3), and aR(5,1) transitions. The data used to calculate the gain on each transition is listed in Table 2.1. The spectroscopic information is known to high precision and the calculated thermal populations have an accuracy of a few percent. The major limitation to the accuracy of the gain calculations is the uncertainty in the population relaxation rates γ_0, γ_1, and γ_2, and in the transverse relaxation rate γ_{12}. The pressure broadening coefficients γ_{01} and γ_{02} are known to an accuracy of about 10%, but very few of the other relaxation rates have been measured. In microwave experiments, the rate γ_1 for the s(8,7) level has been found to be approximately equal to γ_{01}.[23] In the $\nu_2 = 1$ level γ_0 is much slower.[24,25] The strongest form of collisional coupling is to the inversion level of the same rotational state. The inversion energy separation is 45 times larger in the $\nu_2 = 1$ level than in the ground level, so the upper states do not couple as effectively to one another and the relaxation rate is only about one quarter that of the ground level. For K=0 there is no inversion splitting, consequently the population relaxation rates γ_1 and γ_2 will be slower than for other values of K. Rolland *et al.* found that to describe the saturation behavior in the sP(7,0) laser it was necessary to use a rate $\gamma = \gamma_1 = \gamma_2$ about half that given by the pressure-broadening coefficient.[26] There is no reliable information on the rate γ_{12} for any value of K, so it is assumed to satisfy

$$\gamma_{12} = \frac{\gamma_1 + \gamma_2}{2} .$$

The large uncertainty in γ_{12} has its greatest effect on the saturation behavior of the 12-μm gain. Decreasing γ_{12} by 50 % does not

TABLE 2.1

Spectroscopic data used to calculate the 12-μm gain in optically pumped NH_3. The dipole transition moment for the ν_2 transition is 0.24 D.

CO_2 laser transition and pump offset[a]					
00^01 9R(30)	184 MHz	00^02 9P(17)	142 MHz	00^02 9P(7)	87 MHz

NH_3 pumped/lasing transitions and their frequencies[b] (cm^{-1})					
sR(5,0)	1084.629	sR(3,3)	1046.374	aR(5,1)	1054.913
sP(7,0)	827.878	sP(5,3)	867.720	aP(7,1)	798.222

Fractional Populations at T=300K (calculated)		
$n_0 = 1.19 \times 10^{-4}$	$n_0 = 2.73 \times 10^{-4}$	$n_0 = 6.95 \times 10^{-5}$
$n_1 = 7.26 \times 10^{-3}$	$n_1 = 2.14 \times 10^{-2}$	$n_1 = 3.68 \times 10^{-3}$
$n_2 = 1.82 \times 10^{-2}$	$n_2 = 3.20 \times 10^{-2}$	$n_2 = 9.25 \times 10^{-3}$

Fractional Populations at T=195K (calculated)		
$n_0 = 6.46 \times 10^{-6}$	$n_0 = 2.83 \times 10^{-5}$	$n_0 = 4.11 \times 10^{-6}$
$n_1 = 3.35 \times 10^{-3}$	$n_1 = 2.08 \times 10^{-2}$	$n_1 = 1.71 \times 10^{-3}$
$n_2 = 1.63 \times 10^{-2}$	$n_2 = 4.95 \times 10^{-2}$	$n_2 = 8.34 \times 10^{-3}$

a. From Refs. 10 and 21.

b. From Ref. 22.

significantly affect the small-signal gain, but can reduce the 12-μm saturation intensity I_s by about 30 %. Our limited knowledge of γ_{12} therefore makes it difficult to predict the maximum powers that can be produced in a given cavity. The best estimates we have of the unknown relaxation rates are summarized in the formulas listed in Table 2.2. These estimates are used in the gain calculations of this chapter and of chapter 3.

In principle, the Raman gain can be calculated on any pair of coupled transitions in the ν_2 band. The results of calculations on some representative NH_3 transitions are shown in Fig. 2.2. At large pump offsets the gain scales inversely with the square of the offset. For pump offsets less than 100 MHz, the inversion gain (or absorption) combines with the Raman gain, making the gain behavior more difficult to characterize. Figure 2.2a shows the change in the calculated small-signal gain with pump offset if transitions having different values of J are pumped. The variation of gain with J is primarily due to changes in the relative populations in the ground state. The population difference between initial and final states is greatest for the aP(4,0) and aP(6,0) lasers, so they show the largest gain at any given offset. The effect of pumping levels that have different values of K is illustrated in Fig. 2.2b. This variation can be accounted for by the J^2-K^2 dependence of the dipole transition element, and the greater degeneracy of the ortho (K=3n) levels compared to the para (K=3n ±1) energy levels.

In a high-Q cavity it was found that the threshold for lasing on

TABLE 2.2

Relaxation Rates. a) General relations used to estimate the relaxation rates γ_0, γ_1, γ_2, and γ_{12} from γ_{01} and γ_{02}.

$K \neq 0$	$K = 0$
$\gamma_1 = \gamma_{01}$	$\gamma_1 = \gamma_2 = \gamma_{12} \simeq \gamma_{01}/2$
$\gamma_2 = \gamma_{02}$	$\gamma_0 \simeq \gamma_1$
$\gamma_0 = \gamma_1/4$	
$\gamma_{12} = \frac{\gamma_1 + \gamma_2}{2}$	

b) Pressure broadening rates at temperatures of 300K[a] and 195K[b] for the three lasing systems examined in this work.

Lasing Transition	γ_{01} 300K / 195K (10^6 s^{-1} $Torr^{-1}$)		γ_{02} 300K / 195K (10^6 s^{-1} $Torr^{-1}$)	
sP(7,0)	61	91	56	84
sP(5,3)	138	207	121	182
aP(7,1)	74	110	70	106

a. From Ref. 27.

b. Calculated from the rate at 300K, as the rates scale with T^{-1} (Ref. 13).

FIGURE 2.2 Variation of the calculated small-signal gain coefficients as a function of offset, with an incident 9-μm pump intensity of 500 W/cm^2. Relaxation rates and energy levels are taken from Refs. 22 and 27. The pump offsets of a few of the lasers described in this thesis are indicated by asterisks.

a) Comparison of gain for different values of J when the aR(J,0) line is pumped and lasing is observed on the aP(J+2,0) line.

b) Gain for different values of K when pumping the sR(5,K) transition and lasing on the sP(7,K) transition.

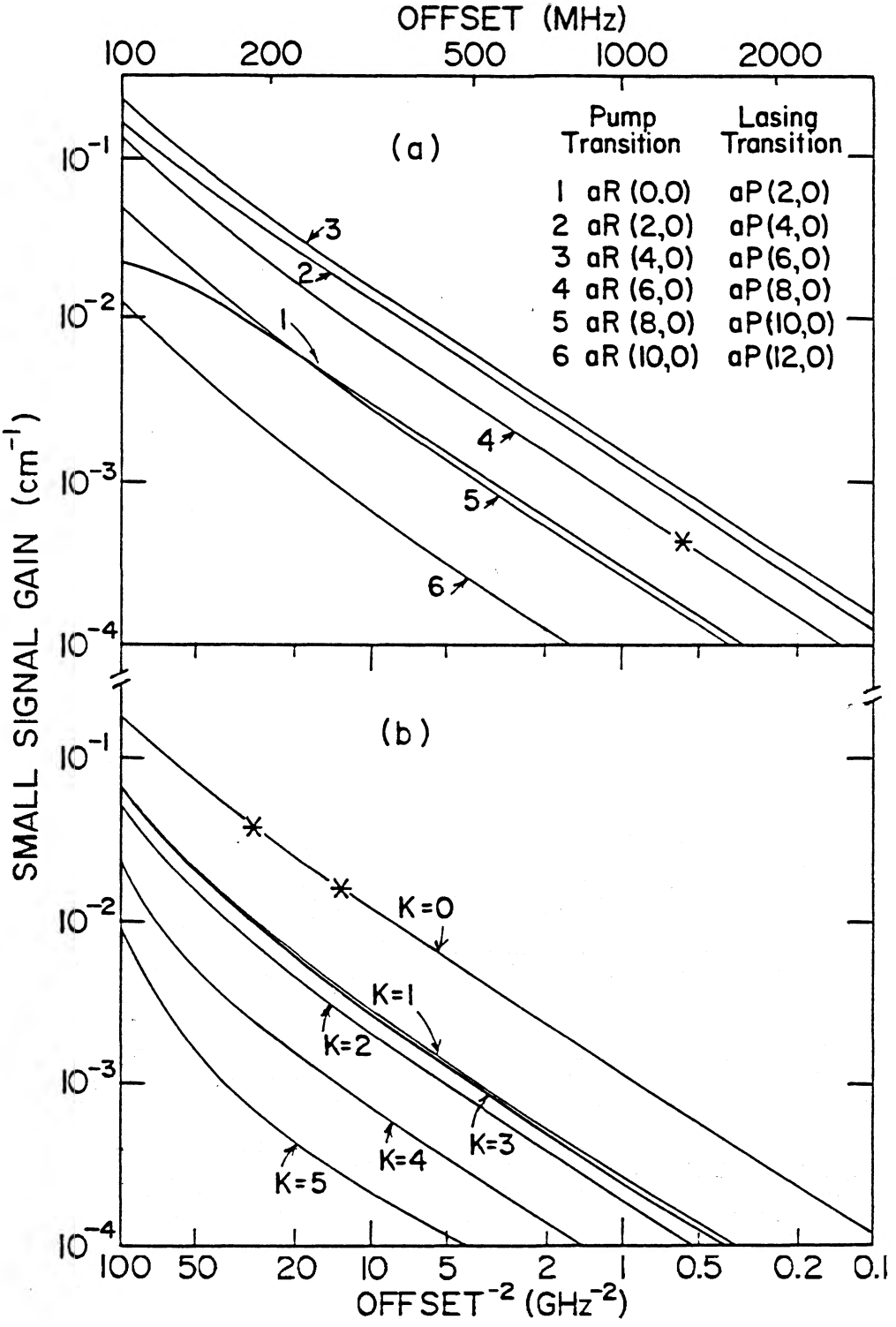
OFFSET (MHz)
100
200
500
1000
2000
(a)
Pump Transition
Lasing Transition
1 aR (0,0) aP (2,0)
2 aR (2,0) aP (4,0)
3 aR (4,0) aP (6,0)
4 aR (6,0) aP (8,0)
5 aR (8,0) aP (10,0)
6 aR (10,0) aP (12,0)
SMALL SIGNAL GAIN (cm⁻¹)
10⁻¹
10⁻²
10⁻³
10⁻⁴
(b)
K=0
K=1
K=2
K=3
K=4
K=5
100 50 20 10 5 2 1 0.5 0.2 0.1
OFFSET⁻² (GHz⁻²)

the aP(8,0) transition occurred at a pump intensity (600 W/cm^2) corresponding to a gain coefficient of $\sim 5 \times 10^{-4}$ cm^{-1}.[28] Taking this gain to be the minimum required, one can use the curves in Fig. 2.2 to estimate the likelihood of lasing for any transition and pump offset.

2.3.2 Inversion Gain

Although there are no exact coincidences of $^{12}CO_2$ laser lines with $^{14}NH_3$ absorption transitions, acousto-optic modulators can be used to shift a pump line into resonance with a nearby absorption line. A cw line-tunable laser has been developed, based on the processes shown in Fig. 2.3. Near-resonant optical pumping of the sR(5,0) transition transfers a sizeable fraction of the NH_3 population from the s(5,0) rotational state in the ground vibrational level to the a(6,0) state in the ν_2=1 level. Dilute mixtures of NH_3 and a non-absorbing gas are used so that collisions with the buffer gas may distribute the population from the upper pumped state to its companion rotational states, and repopulate the lower pumped state. The rotational relaxation rate due to the buffer gas is generally much faster than the vibrational-translational (V-T) relaxation rate.[29] Consequently, the population distribution in the rotational states remains close to thermal equilibrium, i.e., the ratio of the populations in any two states in the same vibrational level is the same as it would be in thermal equilibrium at the ambient gas temperature. However, it has been found experimentally that, when NH_3 collides with either Ar or N_2, the following changes take place: $\Delta J = 0, \pm 1$ and $\Delta K = 0, \pm 3$.[30,31]

FIGURE 2.3 Spectroscopy and energy levels of NH_3 relevant to line-tunable laser operation. The upper trace is a tunable diode laser scan near 1084.6 cm^{-1} of a mixture of NH_3 and CO_2 (From Ref. 19). The scan shows the proximity of the CO_2 9R(30) line to the sR(5,0) and sR(5,1) transitions in NH_3. The lower figure is a partial energy-level diagram of NH_3, showing several P-transitions which have been observed to lase when the sR(5,0) transition was pumped. For simplicity, only K=0 levels are shown. The curved arrows represent the collisional processes that thermalize the population in the upper and lower levels.

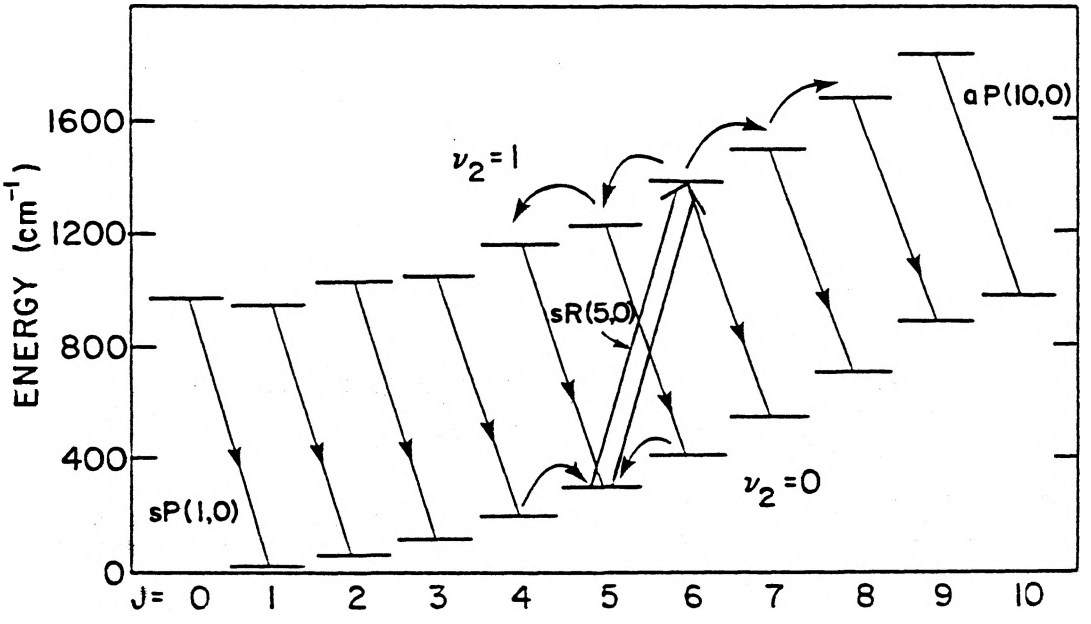
ENERGY (cm^{-1})
1600
1200
800
400
0
J= 0 1 2 3 4 5 6 7 8 9 10
ν_2=1
ν_2=0
sR(5,0)
sP(1,0)
aP(10,0)

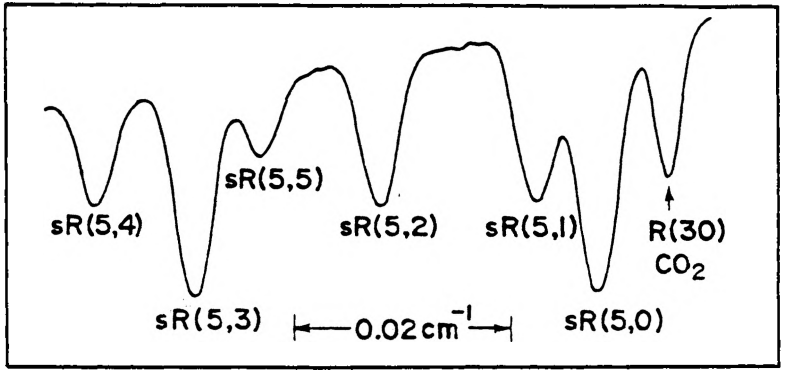
sR(5,4)
sR(5,3)
sR(5,5)
sR(5,2)
sR(5,1)
sR(5,0)
R(30)
CO_2
0.02 cm^{-1}

After multiple collisions J can take on any integer value, but K is more restricted. If a transition with K=0 is pumped, inversion can be created only on transitions with K= 0,3,6,... (ortho transitions). Similarly, pumping a K=1 transition can create gain only on transitions with K = 1,2,4,5,7,... (para transitions). Hence ortho and para NH_3 can be regarded as entirely different species in this laser system. (K = |k|, so pumping a K=1 transition pumps k = ±1, which accounts for the gain being created on K = 2, 5, etc.)

A computer model has been developed that calculates the gain on any line in the ν_2 vibrational band of NH_3. Ortho- and para-NH_3 are considered separately, each with one half the total population. The model considers only the ν_2 = 0, 1, and 2 levels and their respective populations N_0, N_1, and N_2.[17] Four rate equations for N_i and for the populations in the two directly pumped rotational states, r_i, are used. To solve in the cw case, the time derivatives of population are set to zero and a root-finding method is used to determine N_0, N_1, and N_2. The model calculates the ratio N_1/N_0, which descibes the degree of vibrational inversion produced by the pump. The value of N_1/N_0 is then entered into a second program, which calculates the gain coefficients for specific transitions. For simplicity, the populations in the rotational levels are assumed to follow a thermal distribution at the ambient gas temperature. Experimental measurements of gain coefficients, using a tunable diode laser, have been found to be in excellent agreement with the predictions of the model.[29] There is a minor discrepancy between the predictions of the simple model and the

measured gain coefficients on transitions involving the upper or lower pumped states. A 10 % excess (deficit) in the population of the upper (lower) pumped state is sufficient to account for the difference. The presence of a population spike (hole) indicates that the assumption of complete rotational thermalization is not always appropriate. However, the accuracy of the model is more than adequate for the purposes of the work discussed in this thesis.

It is of interest to determine the maximum value of N_1/N_0 that can be attained when a specific transition is pumped. This value is a gauge of the effectiveness of pumping a specific NH_3 transition to produce a vibrational inversion. The maximum inversion will be produced when the pump absorption is saturated. The rate of pumping from rotational state r_0 to r_1 is

$$W_p \Delta r = (I_p/h\nu_p)\sigma [r_0 - r_1(g_0/g_1)]$$

where I_p is the pump intensity at the frequency ν_p, σ is the absorption cross section, and g_0 and g_1 are the degeneracies of the two rotational levels. If complete rotational thermalization is assumed, then $r_i = f_i N_i$, where f_i is the rotational partition function given in Ref. 13. When saturation is reached, therefore,

$$(N_1/N_0)_{max} = \exp[(E_1 - E_0)hc/kT]$$

where E_i is the rotational energy in level r_i. To first order, $E_1 - E_0 = B[J_1(J_1 + 1) - J_0(J_0+1)]$. Thus the largest values of N_1/N_0 will be produced when an R-transition having a high value of J is pumped. For the sR(5,0) and sR(5,1) transitions, $(N_1/N_0)_{max} = 1.8$ at 300 K and $(N_1/N_0)_{max} = 2.4$ at 200 K. Improvement in lasing performance

should therefore be expected if the ammonia is cooled.

The computer model does not at present describe the behavior of the population inversion and gain in the presence of a strong 12-μm field. Consequently, it cannot be used to predict the saturation intensity or maximum power output from the laser. However, the model was used to predict the threshold gains in the waveguide cavity, and to determine which transitions were likely to lase in a given configuration.

2.4 Summary

The previous sections have presented an overview of the theory that describes the behavior of optically pumped lasers. The theory was the basis for two computer models developed by Morrison[17] and Rolland[18] to calculate gain for either Raman or inversion lasers. The following chapters describe the experiments that were carried out to evaluate the models and to make improvements in the performance of the mid-infrared lasers.

CHAPTER 3

RAMAN LASERS

3.1 Introduction

The operation of a cw mid-infrared laser using the sR(5,0) transition in NH_3 opened up the possibility that cw lasing could be produced if other transitions were used. In pulsed laser experiments, the 9R(30) and 9R(16) lines in the 9-μm band of CO_2 are those most commonly used to optically pump NH_3 lasers. The R(30) line has a frequency offset of 184 MHz from the sR(5,0) transition in the ν_2 band of NH_3, and the R(16) line is offset by 1.35 GHz from the aR(6,0) transition. In cw experiments, high power and efficiency were achieved by pumping the NH_3 sR(5,0) transition.[9] Despite the large pump offset, lasing was also achieved in a high-Q cavity in which the aR(6,0) transition was pumped. Operation near threshold was obtained with 30 W of pump power.[28] As the Raman gain decreases with increasing pump offset, an improvement in performance can be expected at reduced offsets. Careful comparison of the frequencies of $^{12}CO_2$ and $^{14}N_2O$ laser lines with those of $^{14}NH_3$ transitions disclosed only two suitable coincidences within 180 MHz. The 9P(7) and 9P(17) sequence lines of CO_2 have offsets of 87 and 142 MHz respectively from the aR(5,1) and sR(3,3) transitions in NH_3. In pulsed systems, Znotins *et al.* achieved lasing when either of these lines were used to pump NH_3,[21] and Rolland showed

that lasing could be achieved with less than 20 W of pump power.[32]

This chapter describes the experiments which were undertaken to produce cw lasing with a sequence-laser pumping arrangement. When lasing was achieved, the output performance of the two new cw lasers was measured and compared to the performance of the sP(7,0) laser. An experiment was then performed to isolate and determine the effect of the pump frequency offset on lasing efficiency. A conventional cw CO_2 laser can be tuned only about 30 MHz from the gain peak, so an acousto-optic modulator was used to upshift or downshift the frequency of the pump radiation by 90 MHz. The sR(5,0) transition was pumped at frequency offsets of 94 and 274 MHz and the results of output power measurements clearly demonstrated the effect of pump offset on the performance of a Raman laser.

3.2 Sequence Laser Construction

In the mid-seventies, Reid and Siemsen discovered that CO_2 could be made to lase on a pair of sequence bands that parallel the 9.4-μm and 10.4-μm regular bands.[33] Figure 3.1 is an energy-level diagram showing the 9-μm regular and sequence bands in CO_2. In a typical gain cell, a sequence line will have a gain coefficient about half that of its regular neighbours. The larger regular gain prevents any sequence lines from lasing in all but the most selective of cavities. A hot CO_2 cell placed in the laser cavity has been found to produce sufficient absorption on the regular transitions to permit the sequence lines to lase. At a temperature of 630 K, a considerable fraction of CO_2

FIGURE 3.1 Energy level diagram of CO_2 showing the 9-μm regular and sequence bands. The lower levels of the 9-μm lasing transitions are also labelled with the percentage of CO_2 molecules in the level at 630K, to illustrate the effect of the hot cell. The lower (bracketed) number is the percentage of molecules in the level at room temperature, 290 K.

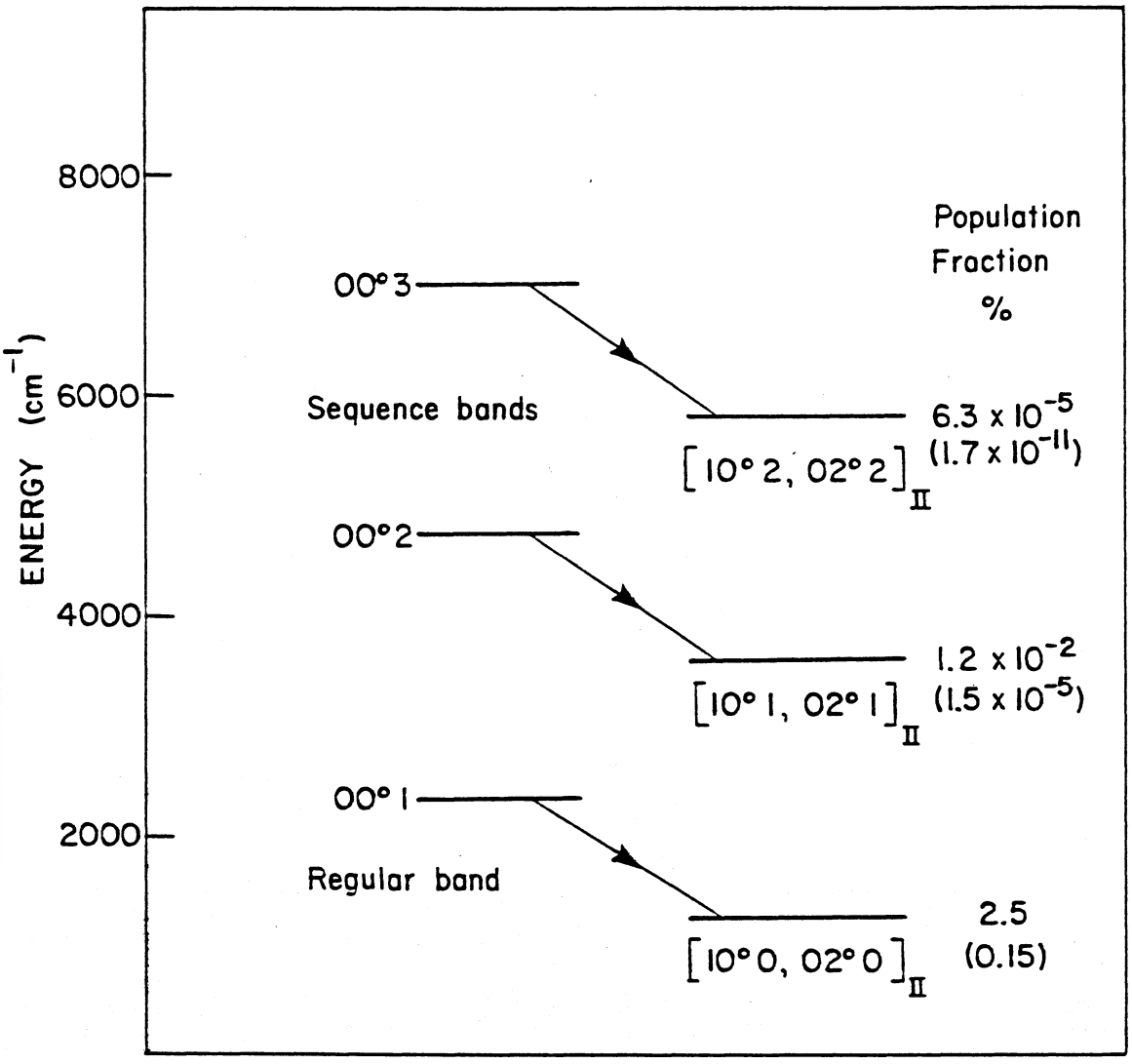
ENERGY (cm⁻¹)
8000
6000
4000
2000
Population
Fraction
%
00°3
Sequence bands
6.3 x 10⁻⁵
(1.7 x 10⁻¹¹)
[10°2, 02°2]II
00°2
1.2 x 10⁻²
(1.5 x 10⁻⁵)
[10°1, 02°1]II
00°1
Regular band
2.5
(0.15)
[10°0, 02°0]II

molecules will be in the $[10^00,02^20]_{II}$ level and therefore produce absorption on the regular 9-μm lines. The populations in the lower levels of the sequence bands will still be small and thus not produce significant absorption. Experimentally, an absorption cell containing 50 Torr of CO_2, and having about one third the length of the laser discharge, is sufficient to ensure lasing on most sequence lines.

The CO_2 gain tubes that were used in this work had discharge lengths of 1.0 to 1.4 m, so a hot cell of effective length ∿43 cm was constructed. The cell consisted of a glass tube of 20 mm i.d., the ends of which were sealed with NaCl windows mounted at the Brewster angle. The cell was electrically heated by a coil of Nichrome wire on the inside surface of the cell, which was wrapped with glass wool insulation to maintain a uniform temperature along its length. Temperature measurements were made along the central axis of the cell with a thermocouple. At typical operating conditions, the temperature was 630 ±20 K over a length of 41 cm.

Typical output powers produced by the sequence laser are shown in Fig. 3.2. At low values of J, the effectiveness of the hot cell absorption diminishes, and regular lines begin to compete with the sequence lines. At high J, the hot cell continues to be effective and lasing occurs only on sequence lines. Some high-J lines exhibit anomalously large powers because there is overlapping gain from higher sequence bands. Of the two sequence lines that were used to optically pump NH_3, the P(17) line had the higher gain, and consequently produced a more powerful and stable output than the P(7) line.

FIGURE 3.2 Typical output powers produced on different CO_2 sequence lines in a laser having a discharge length of 120 cm. The laser was run at a pressure of 17 Torr with a mixture of CO_2:N_2:He content approximately 8:18:74. The powers observed on the competing regular transitions are shown below the axis. The output mirror transmissions were a) 22%, and b) 8% .

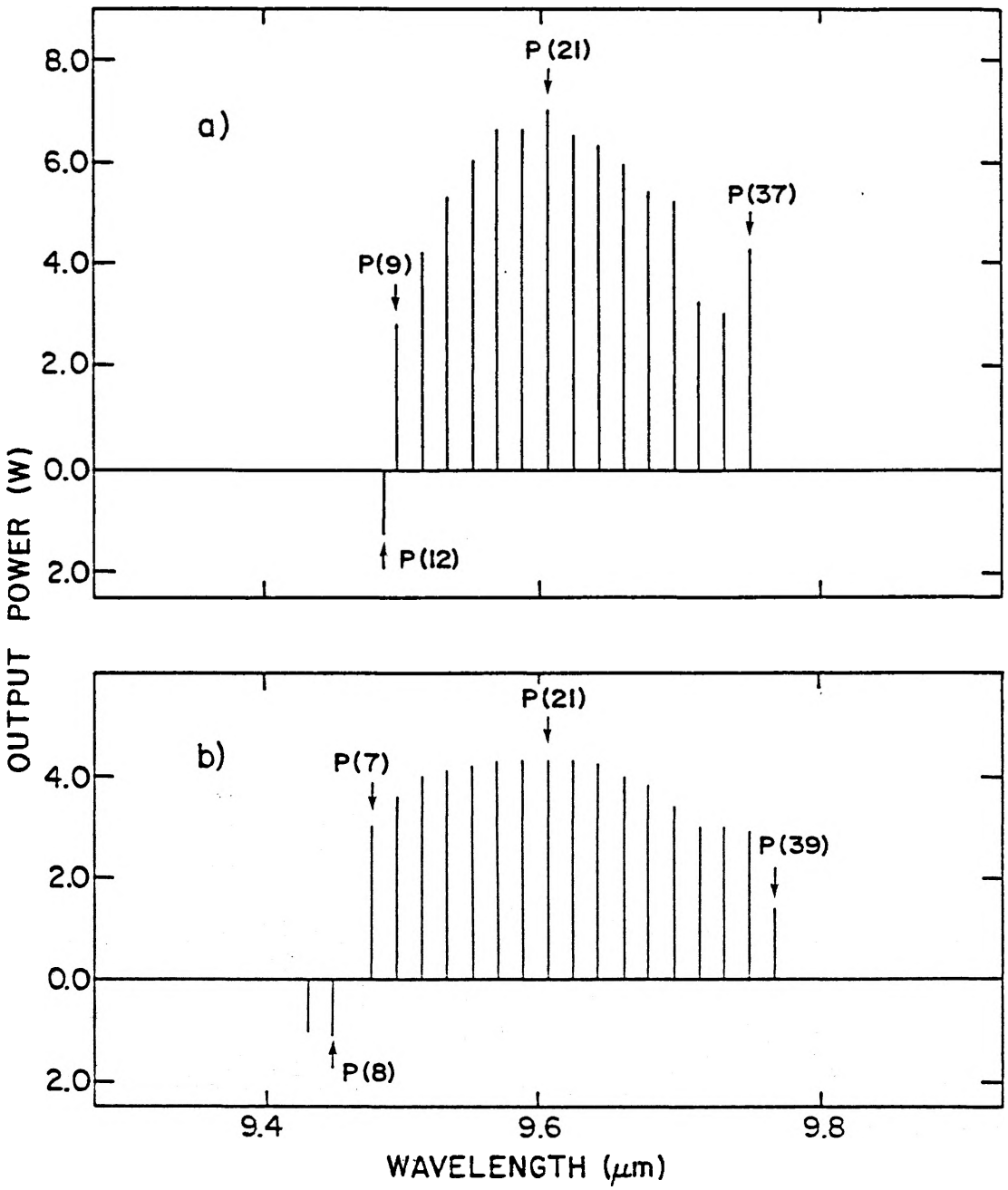
a)
P(21)
P(37)
P(9)
P(12)
8.0
6.0
4.0
2.0
0.0
2.0
b)
P(21)
P(7)
P(39)
P(8)
4.0
2.0
0.0
2.0
9.4
9.6
9.8
OUTPUT POWER (W)
WAVELENGTH (μm)

3.3 Acousto-Optic Modulator Performance

An acousto-optic modulator (AOM) operates by light scattering off a periodic structure in a crystal in a manner similar to diffraction by a grating. Figure 3.3 shows the major features of an AOM. An acoustic (pressure) wave travelling through a solid produces a spatially periodic variation in the index of refraction of the medium, with a characteristic wavelength $\Lambda = v/f$, where v is the velocity of sound in the solid, and f is the frequency of the wave. For a light beam propagating through the medium at an angle Θ_i with respect to the plane of acoustic wavefronts, Bragg diffraction will occur when

$$n \Lambda \sin \Theta_i = \lambda /2,$$

where λ is the wavelength of the light in the medium. For the IntraAction AGM 903 acousto-optic modulator, this condition corresponds to an angle of incidence outside the modulator of about four degrees. Depending on whether the light is incident at a positive or negative angle with respect to the direction of sound propagation, the scattered beam will be shifted up or down by the frequency of the sound wave (see Fig. 3.3a).

The diffraction efficiency of an AOM is proportional to the (linear) acoustic power density P_a/H, where H is the height of the acoustic beam. Consequently, acousto-optic modulators are generally designed with relatively small active areas. The modulators used in these experiments had an acoustic beam height of $\sim$3 mm, so it was necessary to focus a CO_2 beam to ensure that most of the radiation

FIGURE 3.3 Operation of an acousto-optic modulator.

a) Scattering processes in the modulator that increase or decrease the frequency of the deflected beam when the radiation is incident at the Bragg angle, Θ_B.

b) Cross-sectional views of the modulator, showing its physical construction (from Ref. 34). The acoustic wave of height H and wavelength Λ is produced by a piezoelectric transducer mounted on one end of a germanium crystal. To prevent the buildup of standing waves, the acoustic wave is deflected to an absorber after passing through the interaction area. In general there are two output beams produced, with the frequency-shifted beam deflected by $2\,\Theta_B$ from the incident direction.

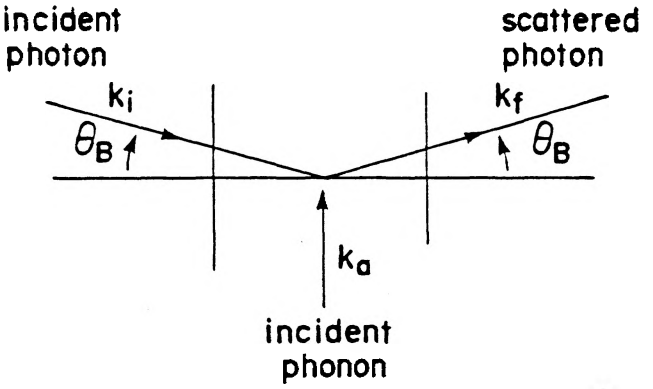

Phonon Annihilation
(frequency upshift)

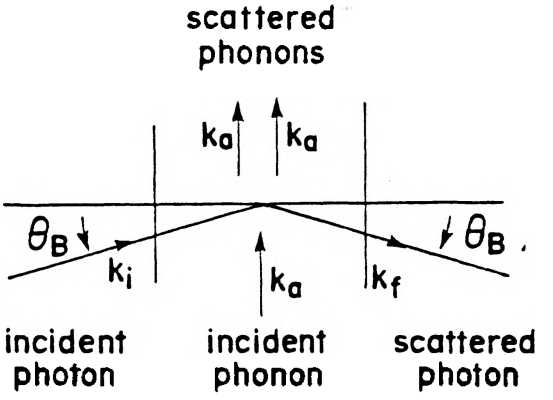

Phonon Creation
(frequency downshift)

(a)

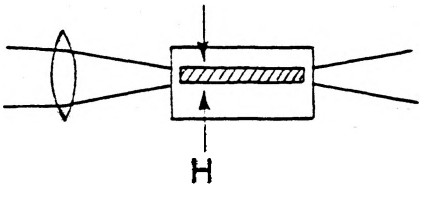

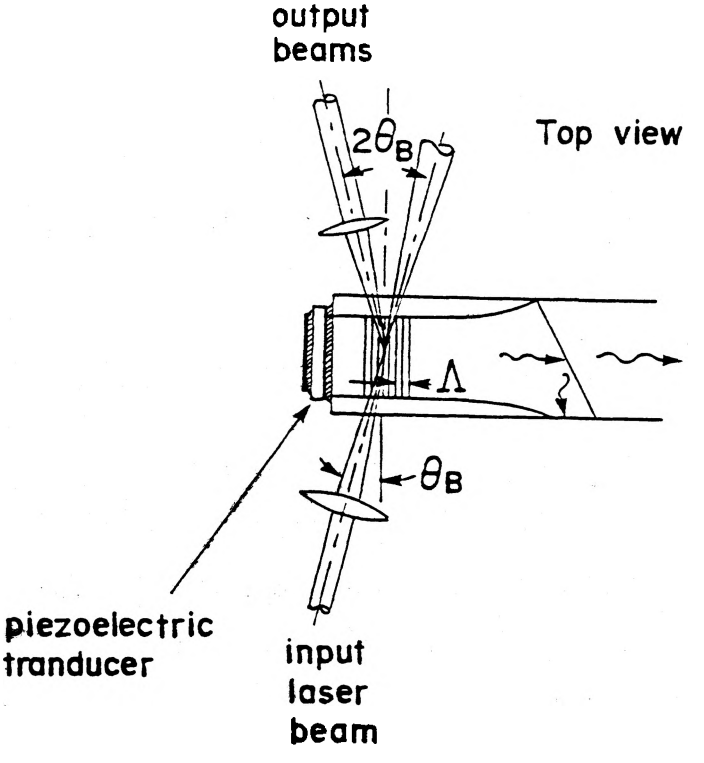

(b)

entered the interaction region. Experimentally it was found that at long focal lengths the beam was apertured vertically by the active region, but with short focal lengths the angular divergence of the beam was too large for the entire beam to be deflected. Maximum power in the deflected beam was achieved when a mirror of focal length 80 cm was used.

Initial measurements of the efficiency of the AOMs were made with a CO_2 laser operating on the 9R(30) line. Initially the laser mode resembled a ring more than a Gaussian spot. Such a mode has a larger spatial extent than a Gaussian beam and is apertured to a greater extent when passing through a modulator. A maximum diffraction efficiency of 50% was observed with the ring mode. Higher efficiencies were observed when the beam took on a more Gaussian appearance, so an aperture was inserted in the laser cavity and several laser tubes of different bore were tested to determine which produced the best output. A tube of 10 mm bore was found to give a good transverse mode structure without sacrificing a great deal of power. Narrower-bore laser tubes generally produced higher powers due to more effective cooling of the laser gases at the walls, but the mode structure of the output beam became more complicated as the diameter decreased. Deflection efficiencies of 56 % per pass were consistently produced with the Gaussian mode. As a final test of the efficiency limitations of the AOMs, the diffraction efficiency of the beam was measured when the radiation was focussed into a modulator by mirrors with focal lengths of 80 and 105 cm. The overall

efficiencies were 56 % and 43 %, respectively. When an aperture was placed at the front of the modulator, and only the central 3-mm-diameter portion of the beam was examined, the efficiencies were 58 % and 64 % respectively. Thus the deflection efficiency of an AOM is limited by the size of its active region.

3.4 Experimental Apparatus and Results

3.4.1 Sequence Laser Pump

Figure 3.4 shows the major features of the arrangement used to optically pump NH_3 with a sequence laser. For stability the sequence laser was mounted on one optical table, which necessitated the use of a bent-cavity configuration. A combination of wire-grid polarizer and Fresnel prism was used to isolate the CO_2 laser from optical feedback.[35] This isolation technique provided the additional benefit of converting the linearly polarized pump radiation into circularly polarized light, which has been shown to produce higher gains in similar optically-pumped systems.[19,35,36] A chopper with a 1/5 duty cycle was used to reduce the average power and prevent damage to the polarizer. All powers have been scaled to cw values. The pump radiation was focussed into a pyrex waveguide set inside a second resonant cavity. The waveguide served to maintain the high intensity of the radiation for a considerable distance without severe loss (Transmission of pump radiation in a 1 m, 2.5-mm bore tube was $\sim$94 %). The circular polarization of the pump and lasing radiation made Brewster windows unsuitable for use in the NH_3 cavity, so the end fittings of the waveguide had slightly-tilted ZnSe windows that

FIGURE 3.4 Schematic diagram of the apparatus used to optically pump NH_3 with a sequence laser. Piezoelectric translators PZT were used to tune the cavity lengths of the pump and waveguide lasers. Dichroic mirrors M_0 reflect $\sim$98 % of incident radiation at 12 μm and transmit $\sim$90 % at 9 μm. Output mirror M_1 was selected for each transition so as to produce the maximum 12-μm output power.

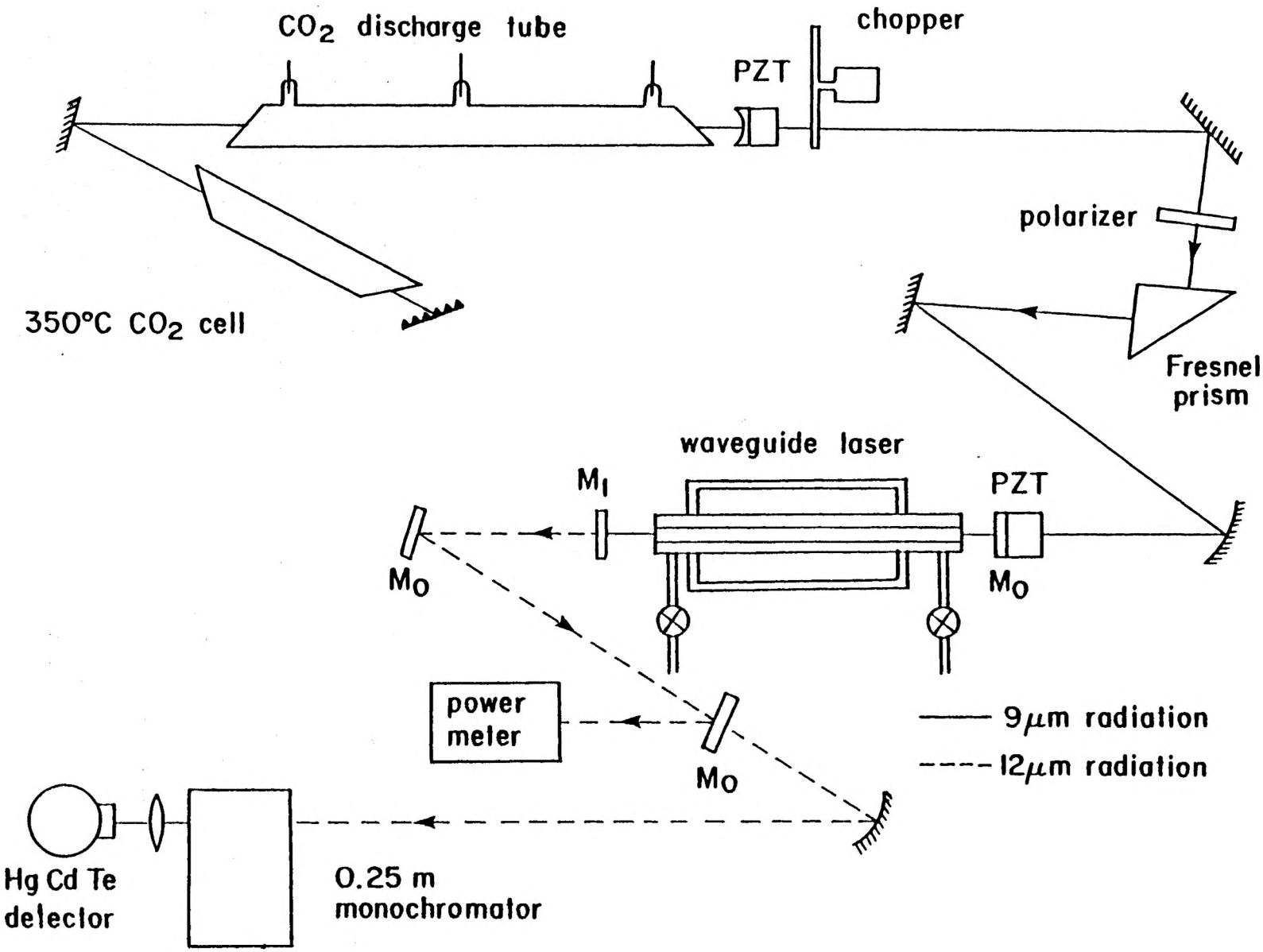
CO_2 discharge tube
chopper
PZT
polarizer
350°C CO_2 cell
Fresnel prism
waveguide laser
M_1
PZT
M_0
M_0
power meter
M_0
9μm radiation
12μm radiation
Hg Cd Te detector
0.25 m monochromator

were anti-reflection coated for 12-μm radiation.

Output from the NH_3 laser was reflected from two dichroic mirrors to eliminate 98 % of the unabsorbed pump radiation and thereby ensure that only the 12-μm power was measured. A calibrated Scientec 365 power meter was used to measure the output power and a 0.25 m monochromator served to isolate and identify the lasing transition. Lasing was detected and optimized by monitoring the signal produced on a HgCdTe detector.

Preliminary measurements were made with a 60cm, 2.5mm-bore waveguide in the NH_3 cavity. Lasing thresholds were determined for the three transitions pumped by the CO_2 regular 9R(30) and sequence 9P(7) and 9P(17) lines. The waveguide was cooled to 200 K by enclosing it in a dry-ice jacket. The cooling served to increase the difference in populations between the initial and final lasing levels in NH_3, and thereby to increase the gain produced.

Table 3.1 lists the results of the threshold measurements. The threshold powers for the sP(7,0) and aP(7,1) lasers agree with the expected scaling of gain with pump offset. The ratio of pump powers (.18) is comparable to the inverse of the squares of their respective frequency offsets (.22). However, the threshold pump power for the sP(5,3) laser is larger than that of the sP(7,0) laser, indicating that such a simple relationship does not generally hold. Different transitions have markedly different relaxation rates and ground state populations, parameters that have a significant effect on the Raman gain. If these additional factors are taken into account, then there is

TABLE 3.1

Lasing threshold powers for a 60cm-long, high-Q NH_3 cavity. A 2.5mm-bore waveguide was used and the cavity was formed by two dichroic mirrors. The waveguide was cooled with dry ice (T=195K).

CO_2 Pump Line	NH_3 Absorption line and frequency[b] (cm^{-1})	NH_3 Lasing Transition and frequency[b] (cm^{-1})	Pump Offset[a] CO_2-NH_3 (MHz)	Threshold Pump Power (W)	NH_3 Pressure (mTorr)
00^02 $P(17)_{II}$	sR(3,3) 1046.374	sP(5,3) 867.720	142	4.0	150
00^02 $P(7)_{II}$	aR(5,1) 1054.913	aP(7,1) 798.222	87	0.4	140
00^01 $R(30)_{II}$	sR(5,0) 1084.629	sP(7,0) 827.878	184	2.5	320

a. From Refs. 10 and 21.

b. From Ref. 22.

good agreement between experimental thresholds and theory. Gain calculations were made using the computer model mentioned in chapter 2 and the data in Tables 2.1 and 2.2. The gain was integrated over the cavity length and over the area of the beam, assuming that the electric fields of the pump and probe beams had a J_0 (zeroth order Bessel function) distribution in the waveguide. Depending on the transition, the calculated gain was 20 to 30 % in the forward direction. An absorption of 5 to 10 % was predicted in the reverse direction, giving a net gain of 10 to 20 %. This net gain is comparable to the losses from the optical elements in the cavity, which amount to about 10 %. The intensity dependence of the gain makes it sensitive to the exact spatial distribution of the pump beam in the waveguide. Thus we estimate that, within the uncertainties of the experiment, the gain calculations agree with the experimental threshold measurements.

To produce the maximum output power from the NH_3 laser, the 60cm waveguide was then replaced with one that was 1 m long. The sequence laser produced 13 W on the P(17) line when an 80 % reflecting mirror was used at the output. This resulted in about 10.5 W incident on the waveguide laser, which produced a maximum output power of 650 mW on the sP(5,3) transition. Optimum power from the NH_3 laser was produced when a Ge mirror with an 83 % reflectivity was used at the output end. The waveguide contained 120 mTorr of NH_3 and was cooled with dry ice. To determine the variation of output power with input power, an absorption cell was inserted in the path of the pump beam and filled with NH_3 to attenuate the pump. Figure 3.5a shows the variation in output power

FIGURE 3.5 a) Variation of output power with input power for the sP(5,3) laser. An output mirror of transmission ∿17 % at 12 μm was found to give the maximum power, at an NH_3 pressure of 120 mTorr.

b) Variation of output with input power for the aP(7,1) laser. Maximum power was produced with an output coupling of 10 % and an NH_3 pressure of 130 mTorr.

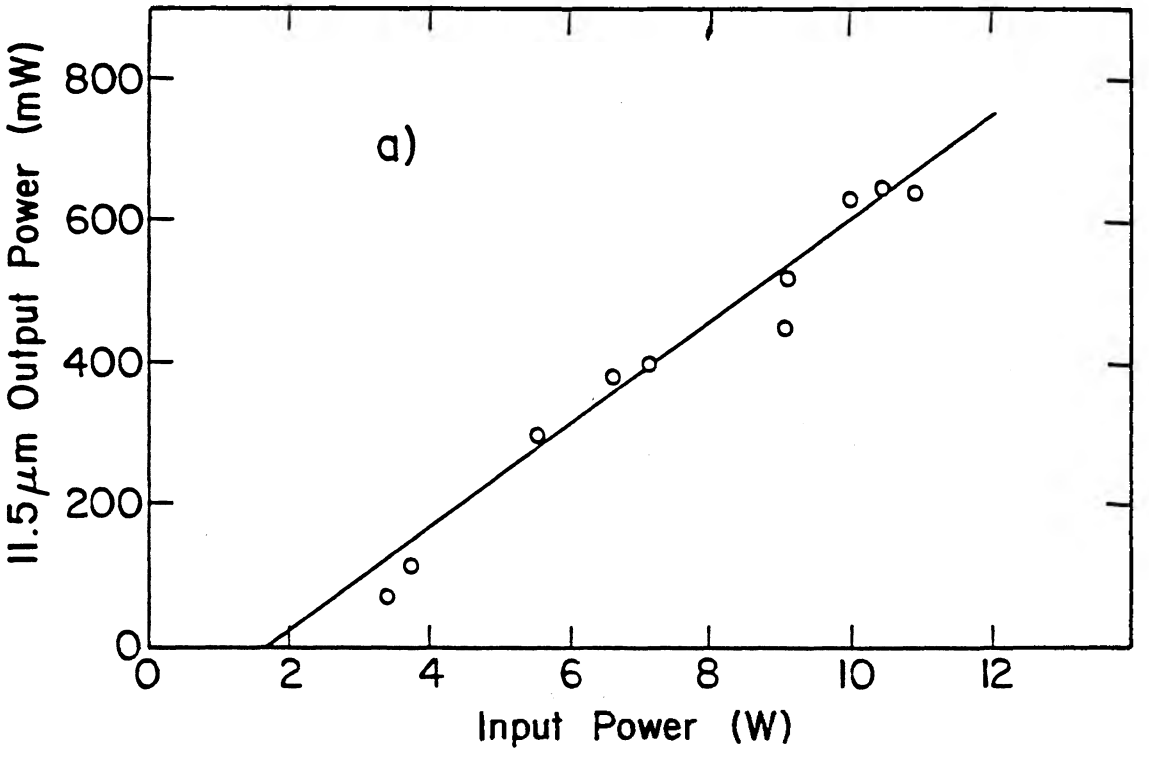
a)
11.5μm Output Power (mW)
800
600
400
200
0
0
2
4
6
8
10
12
Input Power (W)

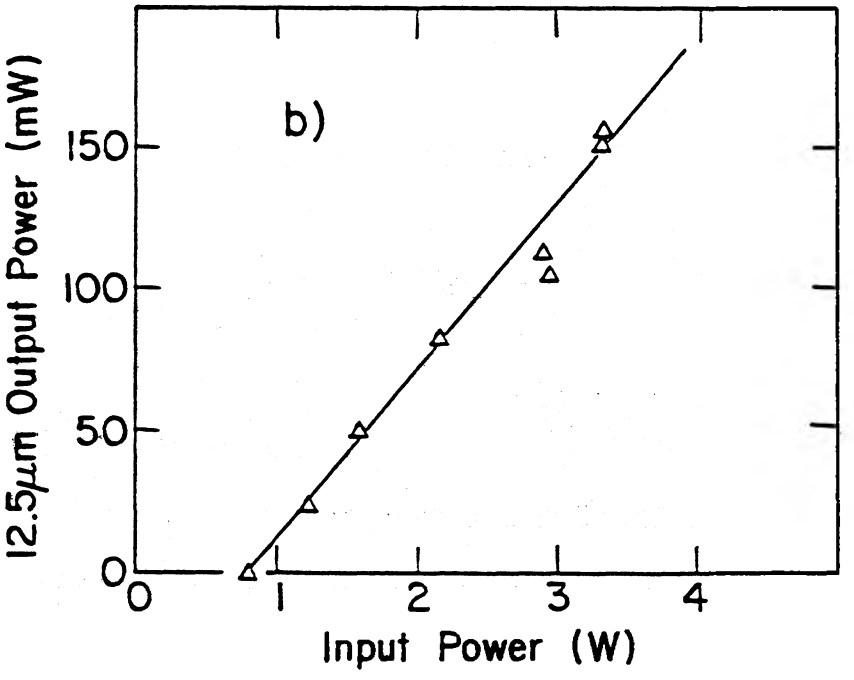
b)
12.5μm Output Power (mW)
150
100
50
0
0
1
2
3
4
Input Power (W)

that resulted. The 11.5-μm power varies linearly with input (slope ∿8 %) and no saturation is evident.

The lower gain on the P(7) sequence line made it necessary to use a 90% reflecting mirror in the CO_2 laser, and 4.0 W of power was obtained. Approximately 3 W was incident on the cooled NH_3 laser and served to produce a maximum output of 155 mW on the aP(7,1) transition. A 90 % reflectivity mirror was used at the output, and the optimum NH_3 pressure was 130 mTorr. The variation of output power with input was measured and is shown in Fig. 3.5b. Again there is no evidence of saturation and the slope efficiency is 6 %.

The output efficiencies of both the sP(5,3) and aP(7,1) lasers are much lower than the 28 % efficiency that Rolland et al. measured for the sP(7,0) laser.[9] Much of the disparity in power output is due to the smaller pump powers available from the sequence laser. However, the lower optimum pressures, which result from pumping at smaller frequency offsets, affect the saturation behavior of the laser and thus limit the output power. The low power conversion efficiencies of the sP(5,3) and aP(7,1) lasers indicate that it may be disadvantageous to operate Raman lasers in pure NH_3 at small pump offsets. To determine clearly the effect of pump offset on laser performance was therefore the objective of the next experiment.

3.4.2 Variable-Offset Pump

To examine the behavior of the NH_3 laser at different pump offsets, the CO_2 9R(30) laser line was chosen to pump ammonia. The

90 MHz frequency shift provided by an IntraAction acousto-optic modulator resulted in pump offsets of 94 or 274 MHz from the sR(5,0) transition. The pumping configuration is shown in Fig. 3.6. An amplifier stage was added to the CO_2 laser to compensate for the losses in the AOM. To prevent thermal damage to the modulator, the 65 W beam was chopped with a 1/20 duty cycle. The CO_2 beam was focussed into the modulator, and the frequency-shifted output directed into the waveguide. The AOM isolated the CO_2 laser from feedback, as any returning light would be shifted an additional 90 MHz from the CO_2 lasing frequency and thus be outside the gain linewidth of the pump laser. A small amount of feedback was observed when the AOM was operating, indicating that the deflected beam was partially reflected at the rear surface of the modulator. (The surfaces of the AOM were AR-coated at 10.6 μm and had 5 % reflectance at 9.2 μm.) The feedback did not seem to affect the stability of the CO_2 laser output, which was dither-stabilized at the gain peak of the CO_2 line.

Initially the AOM was oriented to provide a 90 MHz downshift in the pump frequency. With a pump power of 32 W at an offset of 94 MHz, 6.3 W of output was produced in a dry-ice-cooled waveguide. The output is smaller than that obtained by Rolland *et al.* at 184 MHz offset,[9] but differences in pump polarization and cavity length account for much of the decrease. These differences were not of great concern, as the behavior at a frequency offset of 94 MHz was directly compared to that at 274 MHz.

To pump NH_3 at an offset of 274 MHz, all that was required was a

FIGURE 3.6 Schematic diagram of the apparatus used to optically pump NH_3 at different pump offsets. The acousto-optic modulator (AOM) shifts the frequency of the pump radiation by 90 MHz. The arrow shows the direction of propagation of the acoustic wave in the modulator when a downshift is required. The waveguide was terminated with NaCl Brewster window fittings to minimize the loss in the NH_3 cavity. The mirrors M_0 were dichroic and the output coupler M_1 had a 12-μm transmission of 43 %. Piezoelectric translators PZT were used to optimize power in both the pump and 12-μm lasers.

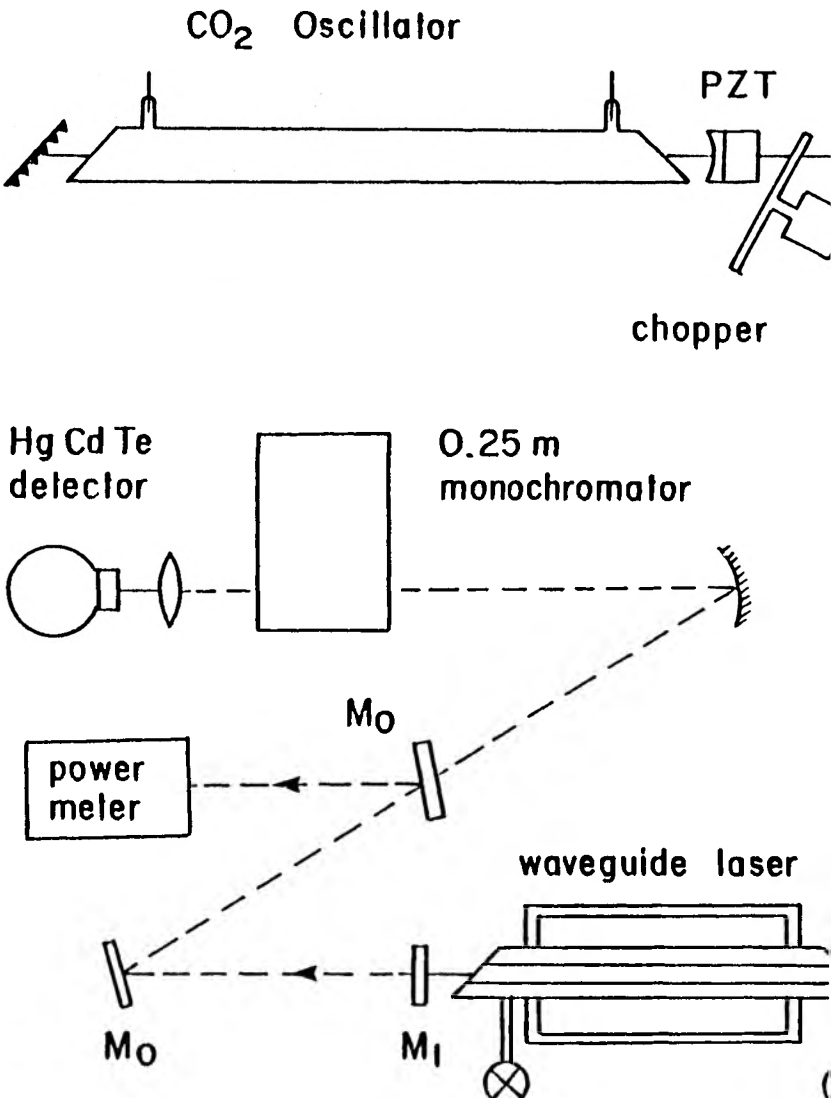
CO_2 Oscillator
PZT
chopper
Hg Cd Te
detector
0.25 m
monochromator
M_O
power
meter
waveguide laser
M_O
M_I

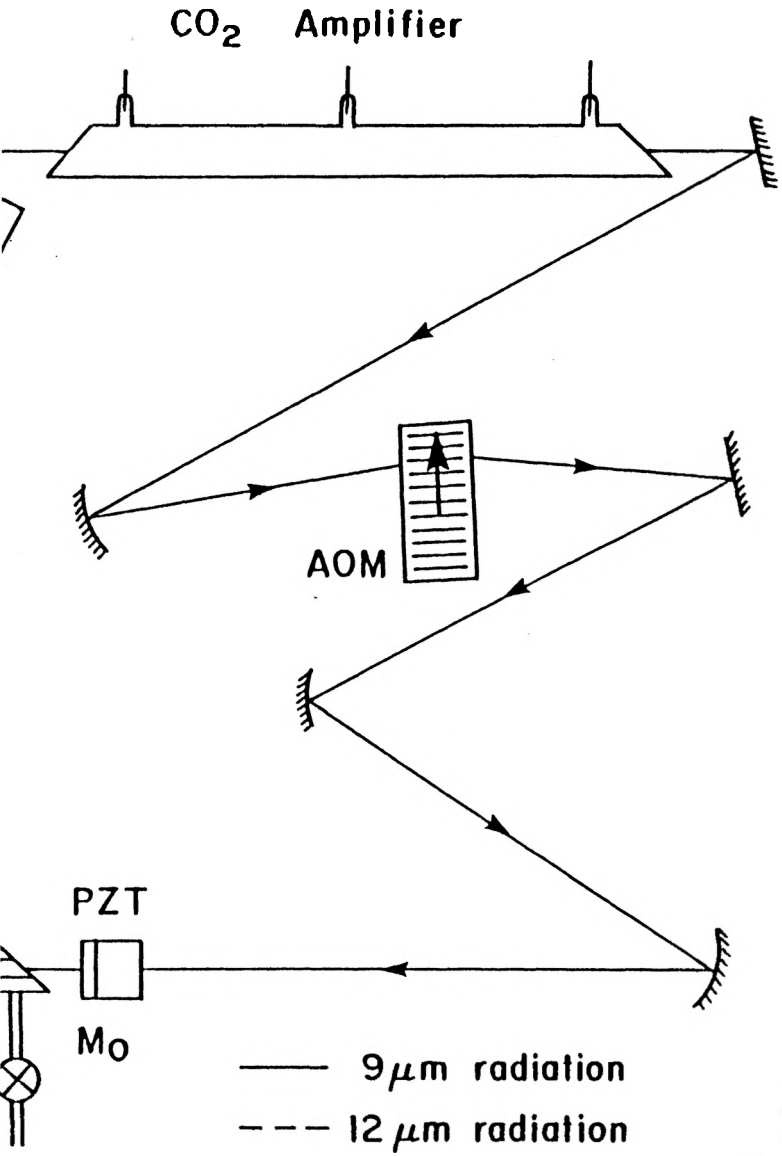
CO_2 Amplifier
AOM
PZT
Mo
9μm radiation
12 μm radiation

rotation of the AOM by 180° . The pump beam followed the same path as before, but was deflected in the opposite direction relative to the AOM acoustic beam. Thus the only change in the experimental conditions was an increase in the pump offset to 274 MHz. A maximum output power of 4.5 W was produced in the cooled waveguide. The graphs of the variation of output with input power for the two offsets have an interesting feature. For the laser with the 94 MHz offset, the slopes of the graphs correspond to efficiencies of 15 % and 20 % at 300 K and 200 K respectively. The slopes of output curves for the laser with the 274 MHz offset were 28 % and 30 %. Two of the curves are shown in Fig. 3.7. The difference in the slope efficiencies is directly related to the optimum operating pressures of NH_3, which were (cold / warm) 240 / 360 mTorr at 94 MHz offset and 440 / 700 mTorr at 274 MHz. As the pump offset is increased, the small-signal gain decreases and higher pump powers are required to reach threshold . However, wing absorption from the 12-μm transition becomes less important and higher pressures of NH_3 can be used. The molecular relaxation rates in NH_3 increase with pressure, consequently at higher pressure the molecular saturation effects, which tend to limit the 12-μm output power, are not as great. Gain calculations made using the average pump intensity in the waveguide (600 W/cm^2) indicate that, although the small-signal gain at 94 MHz is seven times as large as that at 274 MHz, the saturation (half-gain) intensity I_s is 30 W/cm^2 in the 94 MHz laser and 1200 W/cm^2 in the 274 MHz laser. Thus, higher output powers and efficiencies can be expected in larger-offset lasers, if sufficient pump intensity is

FIGURE 3.7 Variation of 12-μm output power as a function of the CO_2 input power, at pump offsets of 94 and 274 MHz. The 12-μm cavity contained a 1.0m-long, 2.5mm-bore capillary tube and the output mirror M_1 had a transmission of ∿43% at 12 μm. The insert shows the principal NH_3 vibrational-rotational energy levels involved in the laser system.

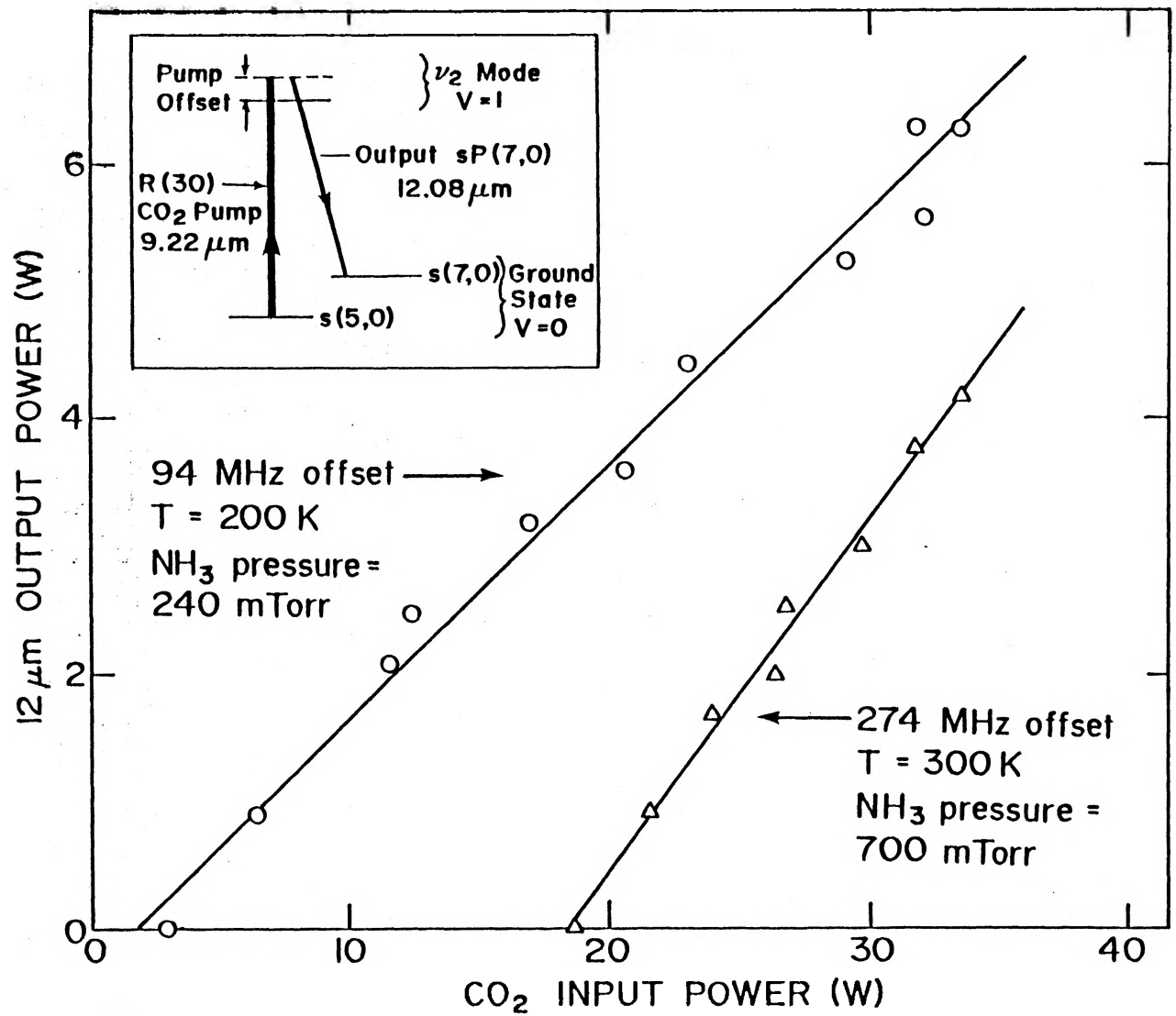
Pump
Offset
ν_2 Mode
V=1
Output sP(7,0)
12.08 μm
R(30)
CO_2 Pump
9.22 μm
s(7,0)
Ground
State
V=0
s(5,0)
94 MHz offset
T = 200 K
NH_3 pressure =
240 mTorr
274 MHz offset
T = 300 K
NH_3 pressure =
700 mTorr
12 μm OUTPUT POWER (W)
CO_2 INPUT POWER (W)
0
2
4
6
0
10
20
30
40

provided.

3.5 Conclusion

Optically pumped cw Raman lasers can operate successfully with pump offsets as large as 1 GHz.[28] In pure NH_3, the 12-μm lasers reach optimum efficiency for pump offsets of 100 to 300 MHz. At large pump offsets (greater than 1 GHz), very little gain is created at intensities that can be produced with a low-pressure CO_2 laser and at small pump offsets (less than 100 MHz), the low operating pressures limit the efficiency of the NH_3 laser. The use of mixtures of NH_3 with a buffer gas would improve Raman lasing at low offsets by increasing the relaxation rates in the vibrational levels. However, at low offsets inversion gain increases in importance and it becomes possible to operate the laser on a large number of transitions in the ν_2 band. NH_3-N_2 and NH_3-Ar mixtures play an important role in the operation of line-tunable NH_3 lasers, which are the subject of the next chapter.

CHAPTER 4

LINE TUNABLE LASERS

4.1 Introduction

Pulsed CO_2 lasers have been widely used to optically pump single transitions in the ν_2 band of NH_3, and generate lasing on many lines in the 12-μm region.[7,8] Recently, this technique has been extended to cw operation by employing acousto-optic modulators to downshift CO_2 radiation into exact coincidence with the NH_3 sR(5,0) transition. This downshifted radiation is a very efficient optical pump of NH_3/N_2 mixtures, and gain can be created throughout the P-branch of the NH_3 ν_2 band. In previous work, lasing was achieved on 20 lines in $^{14}NH_3$, with a maximum output power of 0.7 W and wavelengths ranging from 10.7 to 13.2 μm.[11] All the observed transitions occurred in ortho-NH_3, i.e., all transitions had K= 0, 3, or 6.

In this chapter we describe an improved line-tunable NH_3 laser with cw output powers as high as 5.5 W. The pumping technique has been extended to produce lasing on para-NH_3 lines by pumping the sR(5,1) transition. A total of 65 different transitions with wavelengths from 10.3 to 13.8 μm have been observed to lase.

4.2 Experimental Apparatus

The spectroscopy of NH_3 in the vicinity of the CO_2 9R(30) line

was shown in Fig. 2.3. The frequency offsets of the sR(5,0) and sR(5,1) transitions are 184 and 336 MHz respectively.[10,37] Thus one CO_2 laser line can be used to pump either ortho or para NH_3 if the pump beam is frequency-shifted by 180 or 360 MHz. The experimental apparatus was arranged to achieve the necessary frequency shifts with only one or two acousto-optic modulators. Figure 4.1 shows the initial pumping configuration. The oscillator-amplifier combination provided 65 W of pump power. To prevent damage to the AOM, the beam was chopped with a 5 % or 10 % duty cycle. The pump radiation was focussed into a single AOM, which downshifted the frequency by 90 MHz. A retro-reflector displaced the beam ∿4mm horizontally and sent it back through the modulator. The emerging radiation, downshifted by 180 MHz, was picked off by the edge of a gold mirror. The beam was directed to a second gold mirror, which focussed it into the 2.5-mm bore, 1.0-m long waveguide. NaCl Brewster angle fittings sealed the ends of this waveguide, which contained a mixture of NH_3 and N_2. During an experiment the mixture was flowed at a slow rate to ensure uniform NH_3 concentration, and to allow the pressure to be changed to optimize the performance on each lasing transition.

4.3 Experimental Results: Ortho-NH_3

4.3.1 Non-Selective Cavity

In initial experiments, a two-mirror cavity was used to maximize the output power produced by the NH_3 laser. A dichroic mirror was fixed on a piezoelectric translator (PZT) at the input to the waveguide, and

FIGURE 4.1 Schematic diagram of the apparatus used to produce lasing on ortho- and para-NH_3 transitions in the non-selective cavity. Piezoelectric translators PZTs were used to tune the cavity lengths of the pump and NH_3 lasers. The retro-reflector RR sent the pump radiation back through the acousto-optic modulator AOM. M_0 indicates a dichroic mirror. The output mirror M_1 was selected to give maximum output powers on the lasing transitions and the Freon cell was used to eliminate any residual 9-μm radiation.

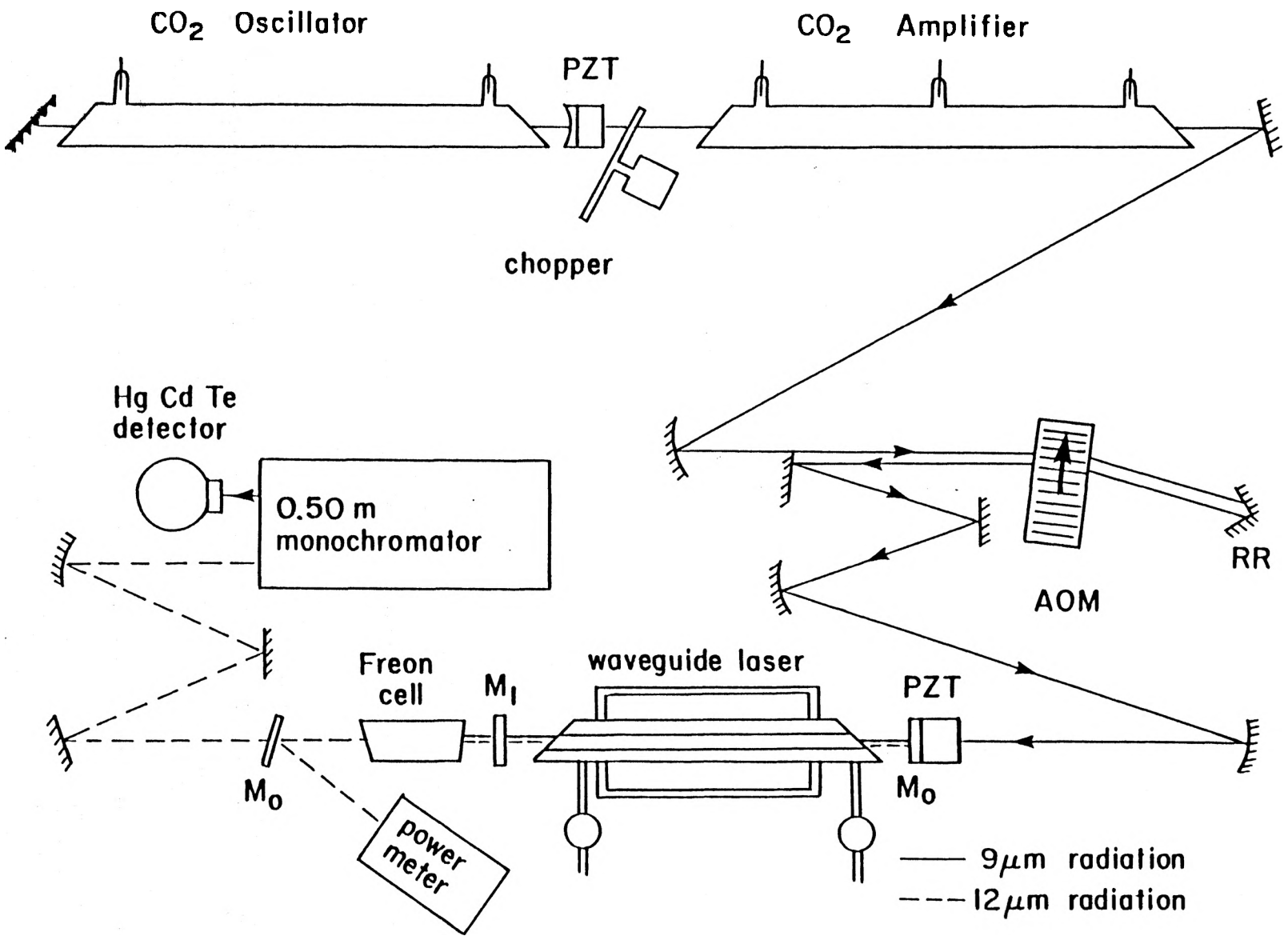
CO_2 Oscillator
PZT
CO_2 Amplifier
chopper
Hg Cd Te
detector
0.50 m
monochromator
RR
AOM
Freon
cell
M_1
waveguide laser
PZT
M_o
M_o
power
meter
9μm radiation
12μm radiation

the 12-μm output was taken from a mirror at the other end of the cavity. The output beam passed through a Freon-12 cell, which removed the residual 9-μm radiation, and was then directed to the Scientec power meter. Identification of the lasing wavelength was made using a 0.5 m monochromator.

To achieve maximum output power, mixtures of 1.0 and 2.0 % NH_3 in N_2 were pumped. The 1.0 % mixture gave higher overall powers, and the maximum output was produced with an output mirror that had a transmission of 43 % at 9 and 12 μm. Approximately 18 W of pump power reached the NH_3 laser after passing through the modulator. At 300 K the laser produced a maximum (multi-line) 12 μm output power of 3.9 W, at a pressure of 5.0 Torr. When the waveguide was surrounded with a dry-ice jacket, the output power increased to 5.5 W, at an optimum pressure of 3.0 Torr. This represents a power conversion efficiency of 33 % and a quantum efficiency of 44 %.

Maximum powers on several strong lines were measured at 200 K. The 12-μm cavity was tuned from line to line by changing the cavity length, which could be varied by several tens of wavelengths by adjusting a differential micrometer on the PZT stage. The operating point for an individual line was chosen so as to minimize the competition from other lines. Output powers obtained on individual transitions are listed in Table 4.1. Although complete isolation of an individual line was not always achieved, for the strongest 5 of the 6 lines that were measured, at least 80% of the total output power was on the transition indicated. On the sP(5,0) and the sP(7,0) transitions,

TABLE 4.1

Observed cw laser transitions in ortho-NH_3. The 9-μm pump power was ∿18 W on the sR(5,0) transition. In all cases the length of the NH_3 cavity was 1.0 m. The relative powers were measured in the grating-tuned cavity and the maximum powers in the two-mirror cavity.

Transition[a]	[cm^{-1}]	Frequency (observed) (±.10 cm^{-1})	12-μm Power Relative[b] (%)	Maximum[c] (W)
sQ(3,3)	967.346	967.18	42[d]	
sQ(4,3)	966.905	966.64	28[d]	
sQ(6,6)	965.354	965.24	43[d]	
sQ(7,6)	964.596	964.37	5[d]	
aR(0,0)	951.776	951.69	28[d]	
sP(1,0)	948.232	948.02	33[d]	
aQ(5,3)	932.992	932.97	30[d]	
aQ(4,3)	931.774	931.69	40[d]	
aQ(3,3)	930.757	930.72	53[e]	
aQ(7,6)	929.162	929.27	10[e]	
aQ(6,6)	927.323	927.39	40	
aQ(9,9)	921.255	921.27	7	
sP(3,0)	908.199	908.23	34	
aP(2,0)	892.156	892.16	44	
sP(4,3)	887.877	887.88	11	
sP(5,0)	868.002	867.99	100	3.1
aP(4,0)	853.818	853.76	75	2.5
aP(4,3)	851.327	851.23	42	
sP(6,3)	847.578	847.63	63	
aP(5,3)	832.635	832.56	49	2.0

Table 4.1 (cont.)

sP(7,0)	827.878	827.90	71	3.5
sP(7,6)	826.470	826.51	5	
aP(6,0)	816.651	816.74	31	1.9
aP(6,3)	814.241	814.36	53	1.2
sP(8,3)	807.472	807.57	9	
sP(8,6)	806.274	806.34	18	
aP(7,3)	796.134	796.17	8	
aP(7,6)	788.510	788.59	13	
sP(9,3)	787.576	787.72	3	
sP(9,6)	786.191	786.22	3	
aP(8,0)	780.568	780.67	13	
aP(8,3)	778.290	778.37	8	
aP(8,6)	770.914	770.99	13	
sP(10,3)	767.809	767.80	<1	
sP(10,6)	766.252	766.20	2	
aP(9,3)	760.694	760.74	11	
aP(9,6)	753.590	753.76	29	
aP(10,0)	745.420	745.50	6	
aP(10,3)	743.307	743.43	4	
aP(10,6)	736.509	736.68	9	
aP(10,9)	723.270	723.31	<1	

a) From Ref. 22.

b) 100 % corresponds to ∿300 mW cw. Unless otherwise noted, the measurement was made in the 2.5-mm bore waveguide at 300K.

c) The maximum powers were measured with an output coupling of 36-43 %. The 2.5-mm bore waveguide, cooled to 200K, was used.

d) Measured in the 1.5-mm bore waveguide cooled to 200K.

e) Measured in the 1.5-mm bore waveguide at 300K.

more than 3W of output power was produced.

To determine the dependence of output power on input power, the pump power was reduced by decreasing the RF power driving the AOM. Figure 4.2 shows the variation of output with input power for both single- and multi-line operation. In each case the output varies linearly with input power and no saturation is evident.

Although it is advantageous to pump close to resonance to obtain maximum inversion of the vibrational levels, inversion can be created with off-resonance pumping. Siemsen et al. observed cw line-tunable lasing with pump offsets as large as 50 MHz (offset from the aR(3,3) transition).[12] In a preliminary experiment it was decided to use a single modulator and pump a 2.0 % NH_3/N_2 mixture at an offset of 94 MHz. A 2.5-mm bore, 1.0-m long waveguide was used and, with an input power of 32 W, lasing was observed on 10 transitions. A 90 % reflectivity mirror was used at the output end. When a 64 % reflectivity mirror was used, a maximum multi-line power of 800 mW was produced. The output power and number of lasing transitions is less than that found in similar conditions when pumping close to resonance. Thus the improved effectiveness of pumping near resonance more than compensates for the the loss from an additional pass through the modulator.

4.3.2 Grating-Tuned Cavity

The substantial improvement in power obtainable on individual lines in the line-tunable NH_3 laser should be accompanied by an increase in the number of transitions on which lasing can be achieved in a

FIGURE 4.2 Variation of the 12-μm output power as a function of the input power pumping the sR(5,0) transition on resonance. A 1.0% NH_3/N_2 mixture at a pressure of 3.0 Torr was used in a 1.0-m long, 2.5-mm bore waveguide. The output mirror had a transmission of ∿43%.

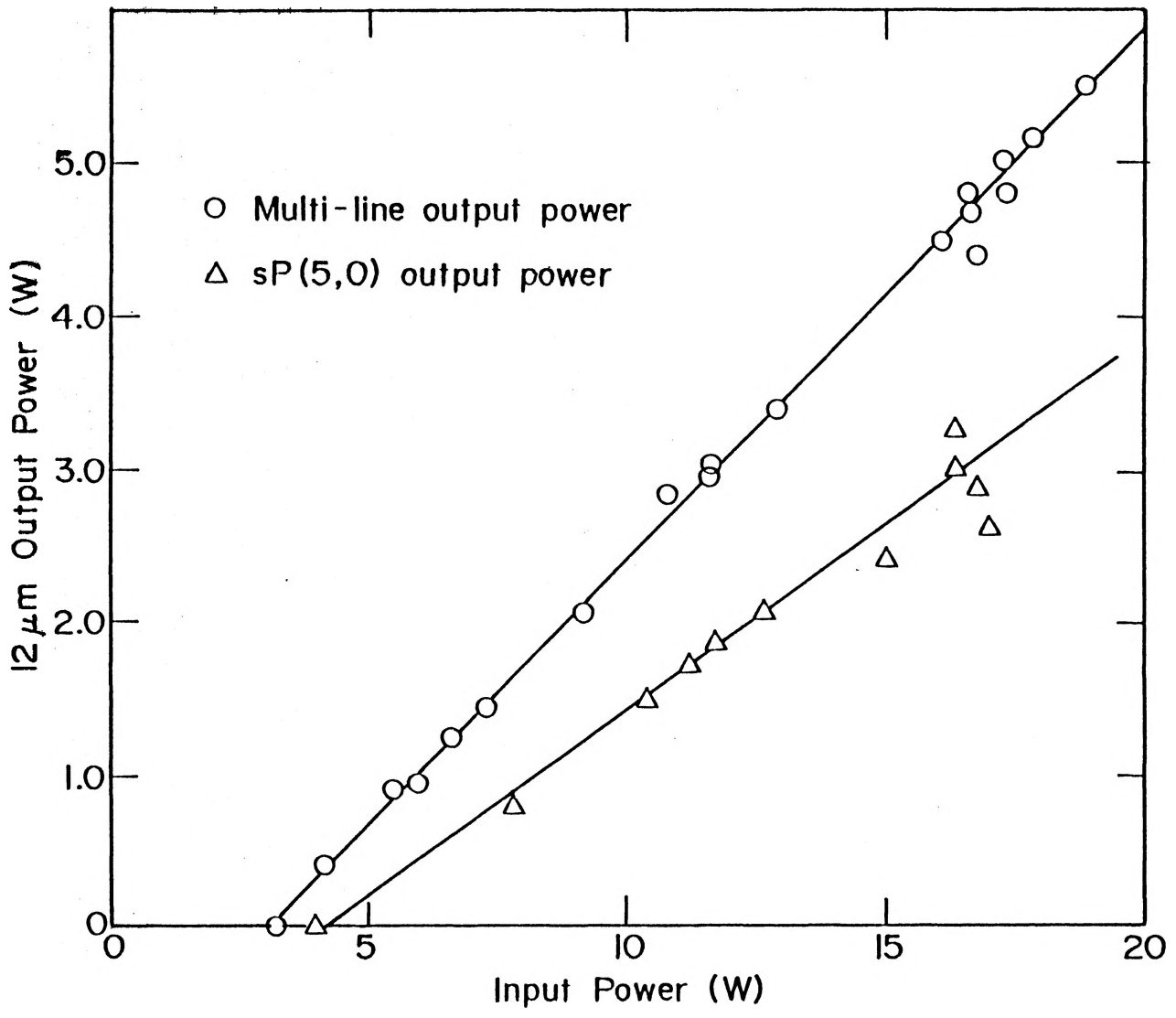
Multi-line output power
sP(5,0) output power
12 μm Output Power (W)
Input Power (W)
0
1.0
2.0
3.0
4.0
5.0
0
5
10
15
20

grating-tuned cavity. To verify this expectation, we replaced the output mirror of the NH_3 cavity with a 12-μm grating (79 lines/mm 35° blaze). The dichroic mirror then served as both the input and the output coupler (see Fig. 4.3). A second dichroic mirror was used to direct the output to the 0.5 m monochromator and the detector. The performances of 0.5 % and 1.0 % NH_3/N_2 mixtures were compared to determine if improvements in line tunability could be made by operating at higher pressures. The 0.5 % mixture proved to be significantly better, and lasing was observed at room temperature on 31 different transitions (see Table 4.1). Optimum pressures for lasing varied from 5 to 8 Torr, generally increasing as higher-J transitions were examined. When a 0.5 % NH_3/Argon mixture was used, a few more high-J transitions were observed to lase. This improvement may be attributed to the slower V-T relaxation rate of NH_3 in argon compared with the rate of NH_3 in N_2.[38] The rotational relaxation rate due to argon is also slower.[17] Hence, in argon mixtures the optimum operating pressures are higher than those found in N_2 mixtures, and larger gain coefficients are produced on all transitions.

Gain on the Q and R transitions in NH_3 is particularly sensitive to the ratio N_1/N_o, which is determined by the pump intensity. Changing the 2.5-mm bore waveguide to one of 1.5-mm bore increased the average pump intensity by a factor of 3. This gave much better lasing performance on the Q-branch transitions, but several of the longer-wavelength lines no longer lased, due to the increased propagation and diffraction losses in the narrower-bore tube. To

FIGURE 4.3 Schematic diagram of the apparatus used to produce line-tunable lasing in NH_3 when grating tunability was desired. (cf. Fig. 4.1) A dichroic mirror M_0 was used as a beamsplitter to direct the 12-μm radiation to the detector.

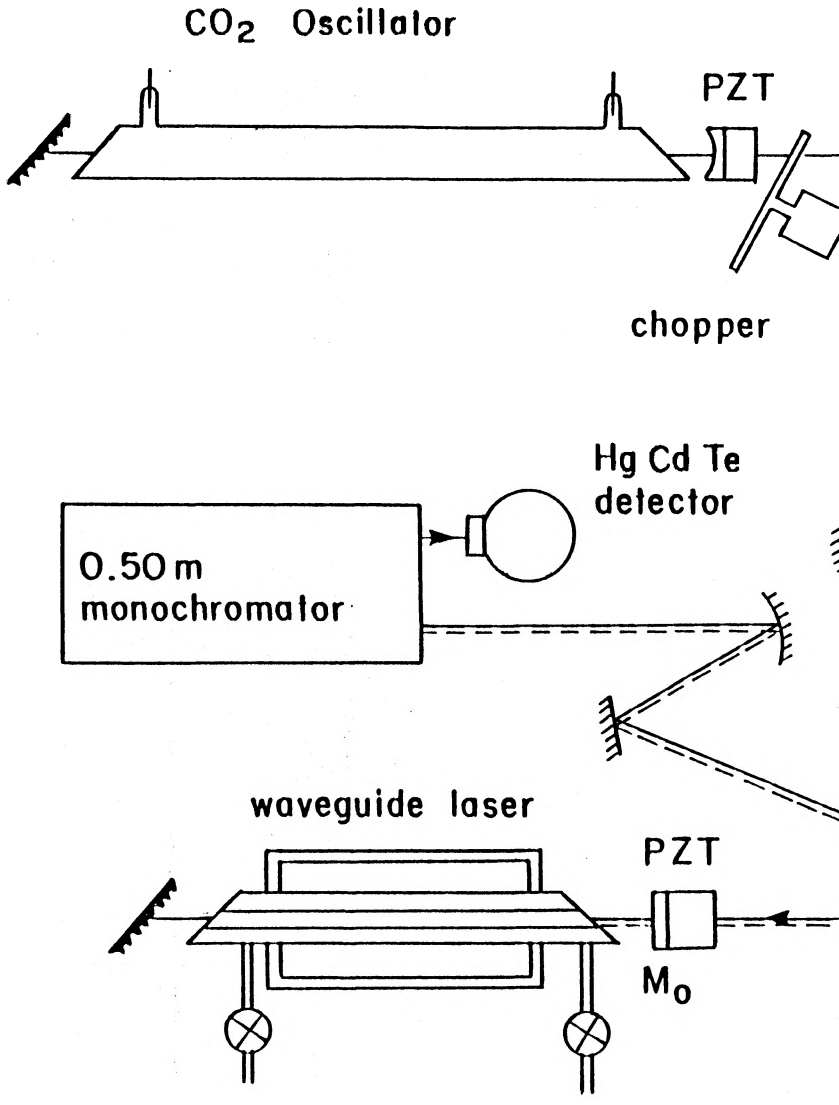
CO_2 Oscillator
PZT
chopper
Hg Cd Te
detector
0.50 m
monochromator
waveguide laser
PZT
M_o

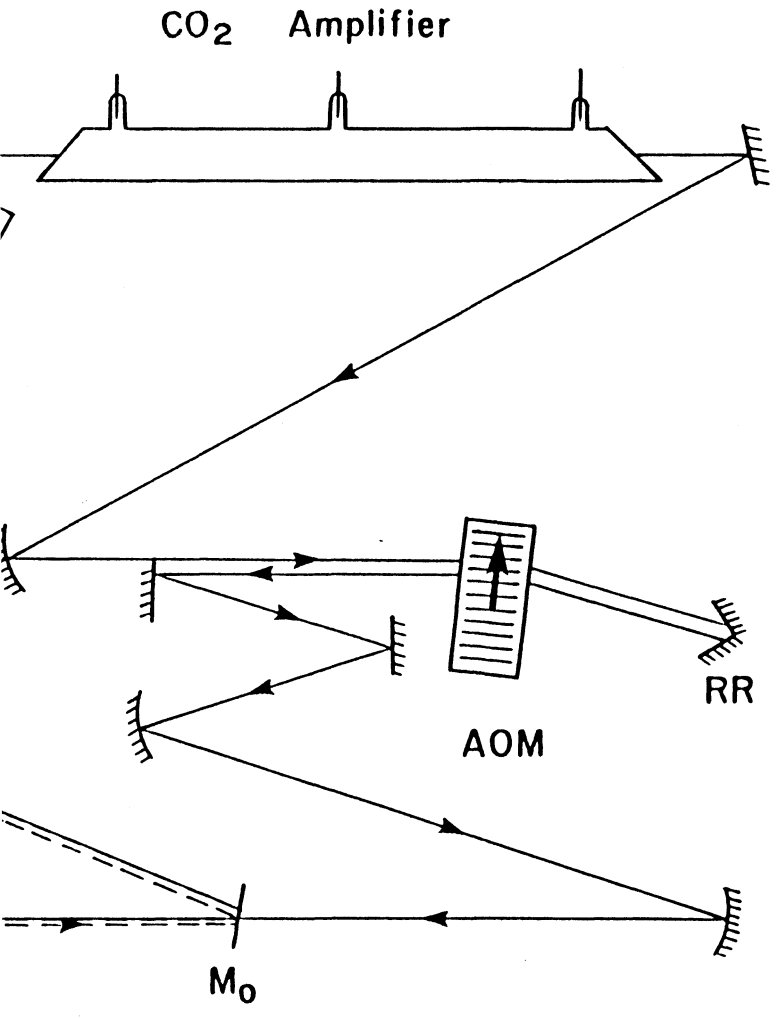

—— 9μm radiation

---- 12μm radiation

further improve the gain on low-J transitions, the waveguide was cooled with dry ice. A 0.5% NH_3-Ar mixture was used, at pressures of 8 to 9 Torr. In addition to observing several new Q lines and the sP(1,0) transition, we achieved the first cw lasing on an NH_3 ν_2 R-branch transition, the aR(0,0) transition. Lasing on an R-transition indicates that there is a high degree of inversion between the ν_2=1 and ground (ν_2=0) vibrational states. For gain to appear on the aR(0,0) transition, the ratio N_1/N_0 must exceed 1.0, i.e., at least half the ortho-NH_3 population must be transferred to the ν_2=1 level.

In total, lasing was observed on 41 distinct ortho transitions. Using the computer model described in section 2.3.2, the gain coefficients on the ortho lines in the ν_2 band were calculated for each of the configurations used. The results are shown in Figs. 4.4 and 4.5. The calculations indicate that a minimum gain of 0.14 % cm^{-1} was required to produce lasing in the 2.5-mm bore waveguide cavity and 0.42 % cm^{-1} in the 1.5-mm bore waveguide. All transitions with gain exceeding loss have been observed to lase, with the exception of a few closely-spaced lines.

The grating-tuned cavity permits much greater selectivity of lasing transitions than does the two-mirror cavity, but the low 12-μm transmission of the input/output dichroic mirror limits the output power. The efficiency of the 12-μm grating was measured in a near-Littrow configuration, using the 12-μm output from the two-mirror NH_3 laser. Approximately 90% of the output was reflected back from the grating. As a consequence of the high grating efficiency, very little

FIGURE 4.4 Calculated small-signal gain for various P, Q, and R transitions in the ν_2 band of NH_3. A 0.5 % NH_3/Argon mixture was used, at a pressure of 8 Torr. The calculation was made for a pump intensity of 234 W/cm^2 on the sR(5,0) transition, indicated by the asterisk. This intensity is the average produced by the 18W pump beam in a 2.5-mm bore waveguide, after losses from the two dichroic mirrors and from coupling into the waveguide are taken into account. The dashed line represents the estimated average loss in the waveguide cavity. The increase in losses at short wavelengths is primarily due to the change in reflectivity of the input dichroic mirror in this region.

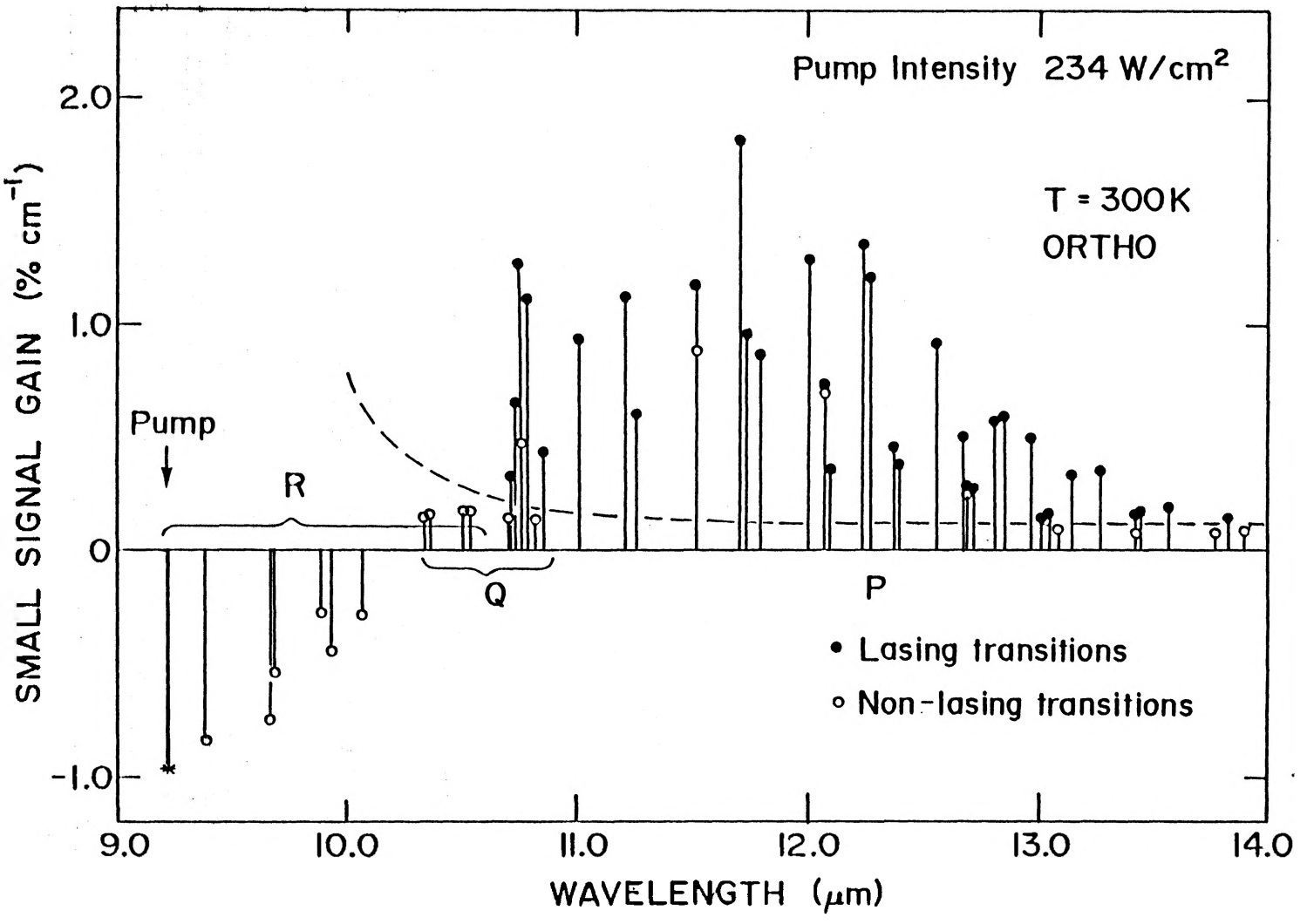
Pump Intensity 234 W/cm²
T = 300K
ORTHO
SMALL SIGNAL GAIN (% cm⁻¹)
2.0
1.0
0
-1.0
Pump
R
Q
P
• Lasing transitions
○ Non-lasing transitions
9.0
10.0
11.0
12.0
13.0
14.0
WAVELENGTH (μm)

FIGURE 4.5 Calculated small-signal gain for various transitions in the ν_2 band of NH_3. A 0.5 % NH_3-Argon mixture at a pressure of 10 Torr was assumed. A pump intensity of 650 W/cm^2 on the sR(5,0) transition was used, corresponding to the average intensity, with losses taken into account, produced in the 1.5-mm bore waveguide. The dashed lines represent the estimated average loss in the waveguide cavity. The insert shows the improvement in lasing performance on low-J transitions when the waveguide was cooled with dry ice.

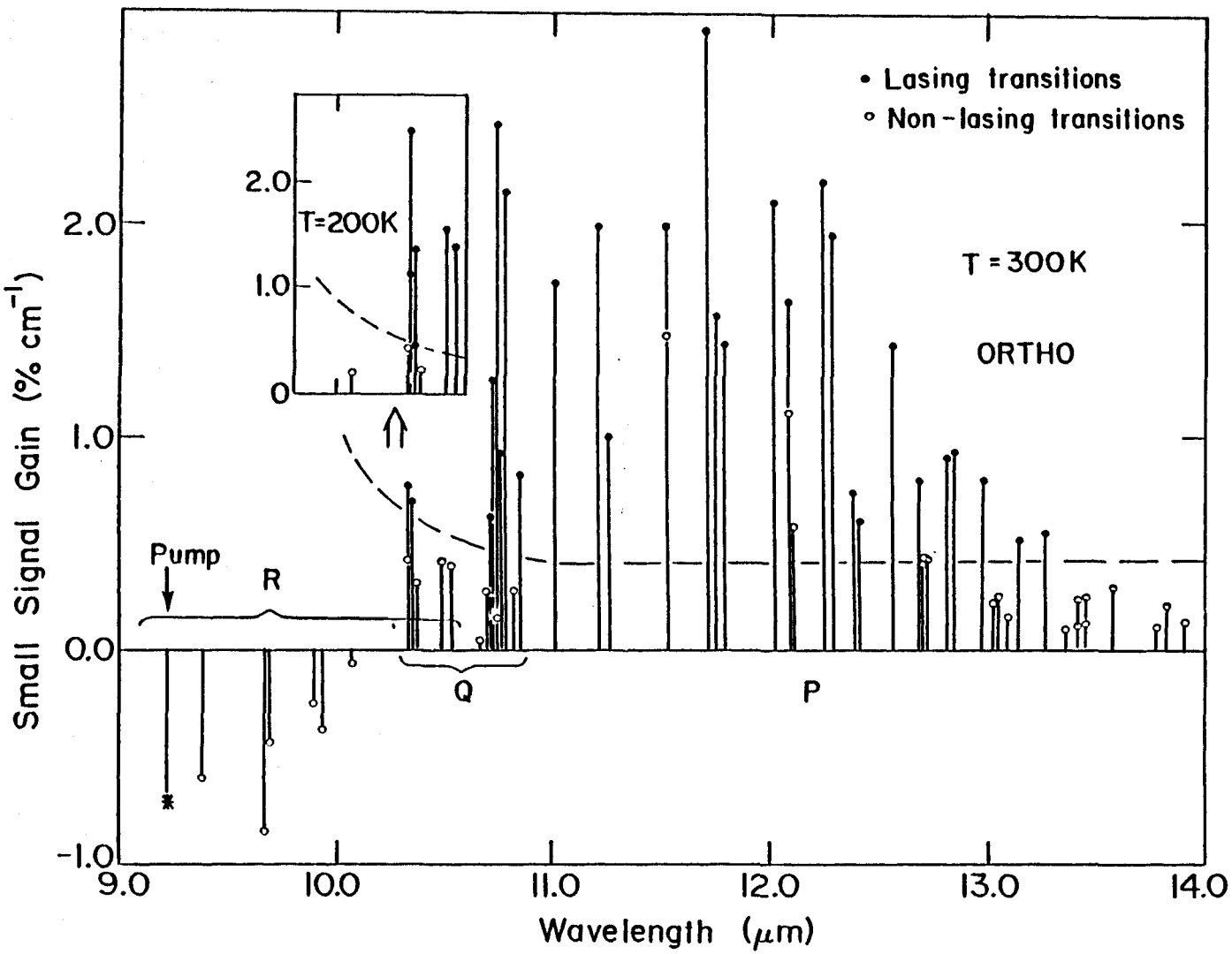
• Lasing transitions
◦ Non-lasing transitions
T = 300K
ORTHO
T=200K
2.0
1.0
0
Pump
R
Q
P
Small Signal Gain (% cm⁻¹)
2.0
1.0
0.0
-1.0
9.0
10.0
11.0
12.0
13.0
14.0
Wavelength (μm)

power was measured in the zeroth order reflection from the grating. Several other gratings were tried, the best of which (PTR ML303, 150 lines/mm) produced about 800 mW of power on the sP(7,0) transition. This is a factor of 3 greater than the maximum power that was obtained when the dichroic mirror served as both the input and output mirror. However, the range of optimum coupling off the grating was limited because the reflectivity of the grating changed considerably over the range of wavelengths used. An additional disadvantage of coupling off the grating is the change in the direction of the output beam whenever a new lasing transition is selected. The best solution to maximizing output power and line tunability would involve changing the input/output mirror of the NH_3 laser. Dichroic mirrors having 12 μm reflectivities of 50 % to 90 % would be needed and the 12 μm grating would be retained at the other end of the NH_3 cavity to provide wavelength selectivity.

4.4 Experimental Results: Para-NH_3

Following successful lasing in ortho-NH_3, the pumping configuration was modified to bring the CO_2 radiation into coincidence with a para transition. A second AOM was inserted before the retro-reflector to provide a total of 360 MHz downshift in the frequency of the R(30) pump. The additional loss in the modulator resulted in only 6 W of 9-μm power being incident on the NH_3 laser, at an offset of about 25 MHz from the sR(5,1) transition. To increase the probability of multi-line lasing we used a 1.5-mm bore waveguide, which maintained an average intensity comparable to that produced in the 2.5-mm bore tube

in the previous experiment. Lasing was readily attained, and a maximum of 240 mW of 12-μm radiation was produced in the non-selective cavity. Maximum output power was achieved with a 1.0 % NH_3/Ar mixture cooled to 200 K and an output mirror transmitting 36 % of the 12-μm radiation. The output powers on several individual transitions are listed in Table 4.2. The power levels are much smaller than those on similar lines in ortho-NH_3 due to the lower pump power and the greater loss in the narrow-bore tube. In a high-reflectivity cavity, a 9-μm power of 1.4 W was required to reach the threshold of lasing on the sP(7,1) transition. The low available pump power is the major factor limiting the cw para-NH_3 laser to low-efficiency operation at present.

In the grating-tuned cavity, only two transitions were observed to lase at room temperature, but dry-ice cooling brought about lasing on a total of 24 para-NH_3 transitions. The relative powers of these lines are summarized in Table 4.2. The computer model can also be used to predict gain on para-transitions. The calculated gain coefficients are shown in Fig. 4.6 for a 0.5 % NH_3-Ar mixture pumped with an intensity of 225 W/cm^2. Once again, a threshold gain of 0.4 % cm^{-1} is required and all isolated transitions with higher gains are observed to lase.

4.5 Conclusions

In this chapter, substantial improvements in the performance of NH_3 inversion lasers are reported. In ortho-NH_3, output powers in excess of 3 W have been generated on individual lines, and power conversion efficiencies of 33% have been achieved in multi-line

TABLE 4.2

Observed cw laser transitions in para-NH_3. The 9-μm pump power was ∿6W on the sR(5,1) transition and all measurements were made using a 1.5-mm bore, 1.0-m long waveguide cooled to 200K.

Transition[a]	[cm^{-1}]	Frequency (observed) (±.10 cm^{-1})	12 μm Power Relative[b] (%)	Maximum[c] (mW)
aQ(2,2)	931.333	931.44	32	
aQ(4,4)	929.898	929.77	100	
aQ(5,5)	928.754	928.62	53	
sP(3,1)	908.177	908.11	59	
aP(2,1)	891.882	891.97	65	
sP(4,1)	888.079	887.96	41	
aP(3,1)	872.567	872.60	43	
aP(3,2)	871.737	871.87	51	
sP(5,1)	867.969	867.91	54	
aP(4,1)	853.548	853.44	39	
aP(4,2)	852.725	852.65	20	
sP(6,1)	847.876	847.79	4	
aP(5,1)	834.824	834.79	27	90
aP(5,2)	834,012	834.03	16	90
aP(5,4)	830.653	830.63	21	
sP(7,1)	827.833	827.94	86	220
aP(6,1)	816.386	816.52	15	50
aP(6,2)	815.591	815.53	34	70
aP(6,4)	812.301	812.30	14	40
aP(6,5)	809.715	809.70	24	

Table 4.2 (cont.)

Transition[a]	[cm^{-1}]	Frequency (observed) ($\pm.10$ cm^{-1})	12 μm Power Relative[b] (%)	Maximum[c] (mW)
aP(7,1)	798.222	798.25	6	
aP(7,2)	797.448	797.55	27	
aP(7,4)	794.244	794.30	14	
aP(7,5)	791.727	791.78	10	

a) From Ref. 22.

b) Relative powers were measured in the grating-tuned cavity. The increase in transmission of the dichroic input/output mirror at frequencies greater than 850 cm^{-1} results in increased relative powers in that region.

c) Maximum powers were measured in a 2-mirror cavity with 35 to 43 % output coupling and 1.0 or 2.0 % NH_3/Ar mixtures.

FIGURE 4.6 Calculated gain on para transitions in the ν_2 band of NH_3 when the sR(5,1) line is pumped. Parameters were set to correspond to a pump intensity of 225 W/cm^2, a temperature of 200 K, and a 0.5 % NH_3-Argon mix at a pressure of 4.5 Torr. The estimated loss line for the 1.5-mm bore waveguide cavity is shown.

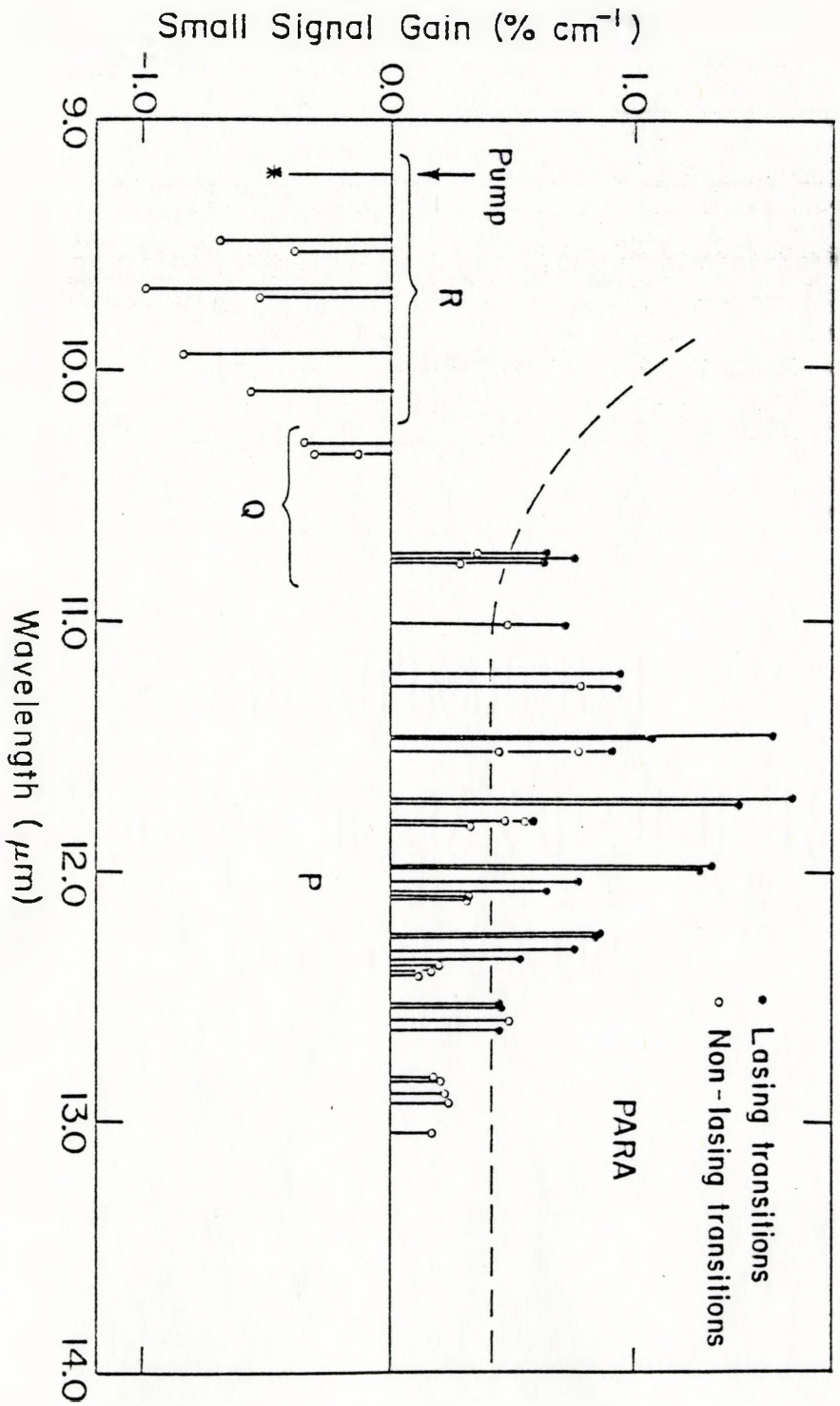
Small Signal Gain (% cm⁻¹)
-1.0
0.0
1.0
9.0
10.0
11.0
12.0
13.0
14.0
Wavelength (μm)
Pump
R
Q
P
PARA
• Lasing transitions
◦ Non-lasing transitions

operation. In addition, we have produced the first cw line-tunable operation on para-NH_3 transitions, making a total (ortho and para) of 65 lines on which lasing takes place in the 10.3 to 13.8 μm wavelength range. In the following chapter, several applications of this laser will be described and future developments of continuous-wave NH_3 lasers will be discussed.

CHAPTER 5

CONCLUSION

This thesis presented the results of several experimental investigations of cw mid-infrared laser systems. Both Raman and inversion 12-μm lasers have been examined and evaluated using computer models of the separate gain processes. Considerable improvements were made in the output power and in the number of wavelengths produced by cw line-tunable NH_3 lasers. In the light of the experimental results, future developments and applications of cw NH_3 lasers will be discussed.

In optically pumped NH_3 lasers, both Raman and inversion processes occur, but at pump offsets significantly greater than 90 MHz only the Raman scattering process generates gain. Prior to the present work, only two cw Raman lasers had been made to operate, with pump frequency offsets of 184 MHz and 1.35 GHz. The initial focus of the present work was the construction of two new cw lasers that were pumped at frequency offsets of less than 150 MHz. Smaller pump frequency offsets generally imply greater Raman gain for a given pump intensity and therefore lower intensities required to reach lasing threshold. The two new lasers did not conform to this behavior because factors such as the ground state populations and dipole transition elements, which also affect gain, change from one transition to another. A single parameter is not adequate to determine the lasing characteristics of a Raman

system, but detailed computer calculations accurately predict the gain produced for a variety of experimental pumping conditions.

The effect of pump offset was isolated experimentally by pumping a single transition, the sR(5,0) line, at offsets of 94 and 274 MHz. The lasing threshold at 94 MHz offset occurred at a much lower pump power than for the 274 MHz offset, but the power conversion efficiency after lasing had been achieved was significantly higher (30 % compared to 20 %) at the larger pump offset. The output power of the laser is determined by the saturation of the 12-μm gain, which is reached when the pumping rate of the molecules approaches the rate at which molecules repopulate the lower pumped level. This relaxation rate is proportional to the gas pressure. At small pump offsets it is necessary to operate at lower NH_3 pressures, where saturation occurs at lower intensities and the efficiency of the laser is reduced. At larger offsets it is possible to operate at higher pressures, where saturation is not as great. When a sufficiently high pump intensity is used, Raman lasing at frequency offsets greater than 200 MHz can be very efficient.

In chapter 4, an investigation of the performance of the cw line-tunable laser was described. It was found that output powers increased substantially when higher pump powers were used and argon performed somewhat better than nitrogen as a thermalizing gas. Many new cw lines were observed to lase in a grating-tuned cavity, but no one cavity configuration was optimal for all lasing wavelengths. A low-loss waveguide was required for lasing on the long-wavelength, low-gain transitions. In a narrower-bore tube, the higher pump intensities

greatly increased the gain at shorter wavelengths and additional lines were observed to lase. Cooling to 200 K further improved the performance in the 10 to 11 μm region. Prior to the present work, cw line-tunable lasing had been achieved only on ortho-NH_3 transitions. By frequency shifting the CO_2 9R(30) pump radiation into resonance with the sR(5,1) transition, lasing was produced on several para-NH_3 transitions. A total of 65 (ortho and para) transitions have been observed to lase, at wavelengths of 10.3 to 13.8 μm.

The results of chapter 4 clearly demonstrate that high output power and wide line tunability can be achieved in NH_3 lasers. Further developments along the lines of a compact pumping arrangement, in which $^{15}NH_3$ is pumped directly by CO_2 radiation, are expected in the near future, and it is likely that a $^{13}CO_2$ laser will be used with $^{14}NH_3$ in a similar arrangement shortly thereafter. The line-tunable NH_3 laser has already been used to establish secondary frequency standards in the 11 to 13 μm region.[10] The laser would be an exceptionally efficient pump of low-pressure pure NH_3 because it lases at line center of the NH_3 transitions. In principle, any transition that lased in the NH_3 cavity could be used to produce far-infrared lasing. A line-tunable far-IR laser could be made, with output at wavelengths of 50 to 2000 μm.

In summary, the cw NH_3 laser has extended the desirable characteristics of the CO_2 laser to a new range of frequencies. A large number of lasing transitions now cover the 11 to 14-μm wavelength region and powers in excess of 1 W have been produced on several lines. Many of the applications that have been found for CO_2 lasers can now be

considered for NH_3 lasers and serious consideration can be given to the development of cw NH_3 lasers operating in other parts of the infrared.

REFERENCES

1. M.J. Weber, ed., Handbook of Laser Science and Technology, Vol. I (CRC Press, Boca Raton, Florida, 1982).
2. M.L. Baumik, W.B. Lacina, and M.M. Mann, "Characteristics of a CO Laser," IEEE J. Quantum Electron. QE-8, 150-160 (1972).
3. D.T. Hodges, "A Review of Advances in Optically Pumped Far-Infrared Lasers," Infrared Physics 18, 375-384 (1978).
4. R.W. Waniek, "Far-Infrared Lasers - Two Decades of Progress," Laser Focus 19, 79-85 (March 1983).
5. T.Y. Chang and J.D. McGee, "Laser Action at 12.812 μm in Optically Pumped NH_3," App. Phys. Lett. 28, 526-528 (1976).
6. P.K. Gupta, A.K. Kar, M.R. Taghizaden, and R.G. Harrison, "12.8-μm NH_3 Laser Emission with 40-60 % Power Conversion and up to 28 % Energy Conversion Efficiency," Appl. Phys. Lett. 39, 32-34 (1981).
7. S.M. Fry, "Optically Pumped Multi-Line NH_3 Laser," Opt. Commun. 19, 320-324 (1976).
8. K. Midorikawa, K. Shimizu, H. Tashiro, and S. Namba, "High-Power, Line-Tunable $^{14}NH_3$ and $^{15}NH_3$ Lasers," Appl. Phys. B 38, 185-189 (1985).
9. C. Rolland, J. Reid, and B.K. Garside, "10-W cw Optically Pumped 12-μm NH_3 Laser," Appl. Phys. Lett. 44, 725-727 (1984).

10. K.J. Siemsen and J. Reid, "Heterodyne Frequency Measurements of $^{14}NH_3$ and $^{15}NH_3$ ν_2-Band Transitions," Opt. Lett. 10, 594-596 (1985).

11. C. Rolland, J. Reid, and B. K. Garside, "Line-Tunable Oscillation of a cw NH_3 Laser from 10.7 to 13.3 μm," Appl. Phys. Lett. 44, 380-382 (1984).

12. K.J. Siemsen, J. Reid, and D.J. Danagher, "Improved cw lasers in the 11 to 13 μm wavelength region produced by optically pumping NH_3", Appl. Opt. 25, 86-91 (1986).

13. C.H. Townes and A.L. Schawlow, Microwave Spectroscopy (Dover, New York, 1975).

14. G. Herzberg, Molecular Spectra and Molecular Structure: Volume II Infrared and Raman Spectra of Polyatomic Molecules (D. Van Nostrand Company, Inc., New York, 1945).

15. R.L. Panock and R.J. Temkin, "Interaction of Two Laser Fields with a Three Level Molecular System," IEEE J. Quantum Electron. QE-13, 425-434 (1977).

16. J. Heppner, C.O. Weiss, U. Hubner, and G. Schinn, "Gain in cw Laser Pumped FIR Laser Gases," IEEE J. Quantum Electron. QE-16, 392-401 (1980).

17. H.D. Morrison, "Dynamics of Optically-Pumped Pulsed Mid-Infrared NH_3 Lasers," Ph.D. Thesis, McMaster University, (1984).

18. C. Rolland, "Optically-Pumped cw Mid-Infrared NH_3 Lasers," Ph.D. Thesis, McMaster University, (1984).

19. C. Rolland, J. Reid, B.K. Garside, H.D. Morrison, and P.E. Jessop,

"Investigation of cw Optically Pumped 12-μm NH_3 Lasers using a Tunable Diode Laser," Appl. Opt. 23, 87-93 (1984).

20. C. Rolland, J. Reid, B.K. Garside, P.E. Jessop, and H.D. Morrison, "Tunable-Diode-Laser Measurements of Gain in Optically Pumped NH_3," Opt. Lett. 8, 36-38 (1983).
21. T.A. Znotins, J. Reid, B.K. Garside, and E.A. Ballik, "12-μm NH_3 Laser Pumped by a Sequence CO_2 Laser," Opt. Lett. 5, 528 (1980).
22. R.L. Poynter and J.S. Margolis, "The ν_2 Spectrum of NH_3," Mol. Phys. 51, 393-412 (1984).
23. G.M. Dobbs, R.H. Michaels, J.I. Steinfeld, J.H.-S. Wang, and J.M. Levy, "Transient Effects in Time-Resolved Infrared-Microwave Double Resonance of Ammonia," J. Chem. Phys. 63, 1904-1919 (1975).
24. M.M.T. Loy, "Observation of Population Inversion by Optical Adiabatic Rapid Passage," Phys. Rev. Lett. 32, 814-817 (1974).
25. S.M. Hamadani, N.A. Kurnit, and A. Javan, "Measurement of Excited State Population Decay Time in NH_3 by Optical Adiabatic Rapid Passage," Chem. Phys. Lett. 49, 277-280 (1977).
26. C. Rolland, B.K. Garside, and J. Reid, "Gain Saturation in cw 12-μm NH_3 Raman Lasers," Appl. Opt. 24, 13 (1985).
27. F.W. Taylor, "Spectral Data for the ν_2 Bands of Ammonia with Applications to Radiative Transfer in the Atmosphere of Jupiter," J. Quant. Spectros. Radiat. Transfer. 13, 1181 (1973).
28. D.F. Kroeker, J. Reid, B.K. Garside, and C. Rolland, "Operation of cw 12-μm Raman Lasers in NH_3 with Pump Offsets as Large as 1.35 GHz," Opt. Lett., in press.

29. R. L. Sinclair, J. Reid, H. D. Morrison, B. K. Garside, and C. Rolland, "Dynamics of the Line-Tunable 12-μm Continuous-Wave NH_3 Laser as Measured with a Tunable-Diode Laser," J. Opt. Soc. Am. B 2, 800-806 (1985).

30. T. Oka, "Microwave Studies of Collision-Induced Transitions between Rotational Levels. V. 'Selection Rules' in NH_3-Rare-Gas Collisions," J. Chem. Phys. 49, 3135-3145 (1968).

31. P.W. Daly and T. Oka, "Microwave Studies of Collision-Induced Transitions between Rotational Levels. VII. Collisions between NH_3 and Nonpolar Molecules," J. Chem. Phys. 53, 3272-3278 (1970).

32. C. Rolland, J. Reid, and B.K. Garside, "12 μm Raman Lasers in NH_3 Pumped by Low-Power CO_2 Laser Pulses," IEEE J. Quantum Electron. QE-18, 182 (1982).

33. J. Reid and K.J. Siemsen, "Laser Power and Gain Measurements on the Sequence Band of CO_2," J. Appl. Phys. 48, 2712 (1977).

34. E.H. Young, Jr. and S.K. Yao, "Design Considerations for Acousto-Optic Devices," Proc. of the IEEE 69, 54-64 (1981).

35. D.K. Mansfield, G.J. Tesauro, L.C. Johnson, and A. Semet, "Effects of Passive Isolation on Several Optically Pumped Far-Infrared Laser Lines," Opt. Lett. 6, 230-233 (1981).

36. S.J. Petuchowski and T.A. DeTemple, "Optimum Emission Polarization and Power Enhancement in Circularly Polarized Optically Pumped Lasers," Opt. Lett. 6, 227-229 (1981).

37. J.P. Sattler, L.S. Miller, and T.L. Worchesky, "Diode Laser Heterodyne Measurements on $^{14}NH_3$," J. Mol. Spect. 88, 347-351 (1981).

38. F. E. Hovis and C. B. Moore, "Vibrational Relaxation of NH_3 (ν_2)," J. Chem. Phys. 69, 4947-4950 (1978).